D. TESTS OF NUCLEAR STRUCTURE IN EXTREME CONDITIONS

In addition to spectroscopy along the proton dripline and in heavy nuclei, sensitive tests of nuclear structure continue to be made across the periodic table. In light nuclei, precise tests of the nuclear shell model at high spin were made which allow the microscopic nature of rotational collectivity to be probed. Superdeformed states have now been found across the periodic table and a rather global picture of their structure and stability is emerging. The superdeformed decay properties change with mass; in lighter systems the "normal" and "highly deformed" structures have considerable overlap, and direct E2 decays dominate, while in heavier nuclei the states become very different and a classical barrier arises which is penetrated by statistical E1 decay. Rather few direct decays were seen still, so the picture continues to emerge. Another area "linking" physics topics which started with different aims is the investigation of neutron deficient nuclei in the gap between near-stability and the newly investigated dripline proton emitters along the proton dripline. In the Au-Pt-Hg region, considerable progress was made in finding a unified picture of co-existing shapes and polarizing orbitals right out to the dripline.

A major campaign was mounted to investigate shell structure in hot nuclei, through a self-consistent, extensive and detailed set of measurements of high energy (> 10 MeV) gamma rays. The program was based on using the ORNL/MSU/Texas A&M BaF_2 array, triggered by the Argonne FMA (to provide mass selection) and by the Argonne/ND BGO multiplicity filter (to provide angular momentum information). Spherical, soft, and well deformed nuclei were investigated, and the mechanism of radiative capture.

The artificial divide between reaction mechanism studies and spectroscopy continues to dissolve, as structural effects frequently determine reaction rates, and specific reactions are used to probe selected nuclear structures. This is especially true very near the Coulomb Barrier. The mechanism of sub-barrier fusion was probed using Gammasphere and the FMA and "Radiative Capture" reactions used to populate interesting states in light and heavy nuclei. The Radiative Capture of heavy ions was explored in light (^{12}C + ^{12}C) and heavy (^{90}Zr + ^{90}Zr,^{89}Y) systems, using the BaF_2 array at ANL and Gammasphere at ANL and at Berkeley.

d.1. First Identification of a $J^{\pi} = 10^{+}$ State in ^{24}Mg

(I. Wiedenhöver, A. H. Wuosmaa, C. J. Lister, M. P. Carpenter, R. V. F. Janssens, H. Amro, J. Caggiano, A. Heinz, F. G. Kondev, T. Lauritsen, S. Siem, A. Sonzogni, M. Devlin,*† D. G. Sarantites,* L. G. Sobotka,* P. Bhattacharyya,‡ and B. A. Brown§)

The nucleus ^{24}Mg contains a sufficiently small number of nucleons that its structure can be calculated with the shell model using the full sd-configuration space. Yet, this nucleus also exhibits collective rotational excitations associated with large, prolate deformations. In this context, the identification of states approaching 12 h, the maximum spin that can be generated within the sd shell, is particularly relevant. Their properties provide an opportunity to test the microscopic basis of collective motion; i.e. either they become less collective than lower lying levels as the number of available configurations within the sd shell decreases, or they maintain their collectivity by gathering strength from sizeable admixtures of configurations from higher lying orbitals, e.g. from the fp shell. Such issues are most readily addressed in light nuclei, where shell model calculations remain tractable.

The study of levels beyond the established $J\pi = 8^{+}$ states in ^{24}Mg is hampered by the fact that they are particle-unbound by energies larger than 5 MeV. In addition, their deexcitation often proceeds through rather complex paths and, as a result, angular correlation studies are difficult and quantum number assignments become problematic. These issues are resolved here in an experiment performed at ATLAS. The experimental setup consisted of five 16×16 silicon strip detectors, located around the target for the detection of alpha particles, and of the Gammasphere array for the coincident detection of gamma rays. Excited states in ^{24}Mg were prepared with the ^{12}C(^{16}O,α)^{24}Mg reaction at a center of mass energy of 26.6 MeV.

The technique for spin determination is based on the observation of the five-fold directional correlation between the beam axis, the two α particles and two photons, which are emitted in the decay path leading from the compound state in ^{28}Si (m = 0) to the ground state of ^{20}Ne. All steps in this decay path must be observed in order to produce a characteristic angular correlation which permits spin determination. In order to obtain these correlation patterns, a new technique was developed that relies on an expansion into coefficients of an orthogonal basis and allows the concentration of the relevant information into only few spectra. The power of the technique as successfully tested on a number of states with spin 6, 7 or 8 in ^{24}Mg. Further analysis then provided the first firm spin and parity assignments for 9 states in the energy region between 15.7 and 20.3 MeV in ^{24}Mg. Of particular importance is a state at 19.2(1) MeV which could be assigned as 10^{+}: this is the first such level in ^{24}Mg.

In order to gain more insight into the properties of the 19.2(1) MeV state, a search was undertaken for any possible gamma-decay branch, as any such transition can be expected to link levels associated with closely related configurations. The gamma-ray spectrum gated on (i) a 19.2 ± 0.15 MeV excitation energy and on (ii) any of the ^{24}Mg transitions below the lowest 6^{+} state is presented in Fig. I-30. Also shown is the corresponding background spectrum. A peak is visible at 5927(5) keV. This energy matches the value expected for the gamma transition linking the new 19.2 MeV, 10^{+} level to the rotational 8^{+} state at 13.212 MeV. The subsequent 5099 keV gamma line deexciting this 8^{+} state is also present in the spectrum. The 5927 keV transition establishes a state at 19.139(5) MeV which matches the energy obtained from the alpha spectrum. Since the uncertainty in the particle channel is ~200 keV, the presence of a doublet of levels cannot, however, be entirely ruled out. Under the assumption that the same state is seen in both decay channels, the measured gamma-alpha branching ratio is $7(3)*10^{-4}$.

In order to explore the nature of the new 10^{+} state further, new shell model calculations were performed using the USD interaction[1] in the full sd-shell basis. The results are compared in Fig. I-31 with the data after subtraction of a rotational energy reference defined as $E_{rot}[MeV] = 0.187 * I(I + 1)$. As can be seen from the figure, these calculations reproduce the overall evolution of the ground state band with spin rather well. In particular, the predicted energy for the 10^{+} level of 19.104 MeV is in excellent agreement with the present measurement. The curvature seen in the figure can be viewed as a signature for the onset of band termination, i.e. the level energy decreases with respect to the rotational reference as one approaches the 12^{+} state obtained by aligning the spins of the eight valence nucleons. In fact, the wave function of the USD 10^{+} state is dominated (50%) by the $(d5/2)^7 \times d_{3/2}$ configuration, which can be interpreted as a particle-

hole excitation built from the 8^+ level which has a 46% $(d_{5/2})^8$ component in its configuration. Thus, the 10^+ excitation energy is largely determined by the effective $d_{5/2}$ - $d_{3/2}$ spin-orbit splitting.

*Washington University, †Los Alamos National Laboratory, ‡Purdue University, §Michigan State University

1B. H. Wildenthal, Prog. in Part. and Nucl. Physics **11**, 5 (1984); B. A. Brown and B. H. Wildenthal, Ann. Rev. Nucl. Part. Sci. **38**, 29 (1988).

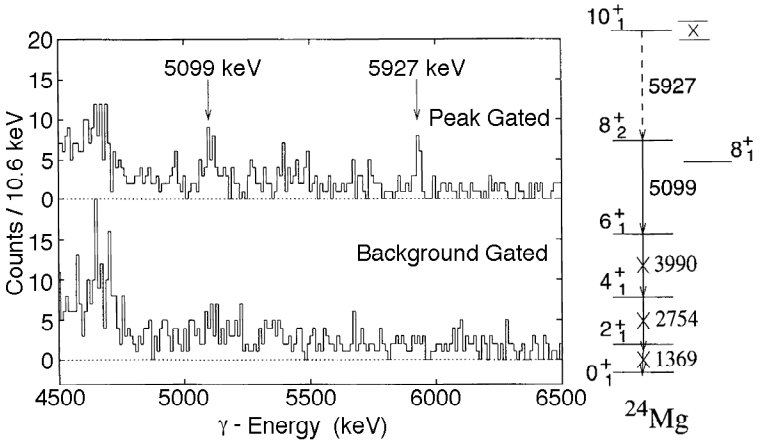

Fig. I-30. Upper part: gamma spectrum gated on a 19.2(15) MeV excitation energy in coincidence of either of the 1369, 2754 or 3990 keV ground state band transitions. The decay scheme illustrates the gating conditions with a cross. Lower part: gamma-spectrum gated on background regions.

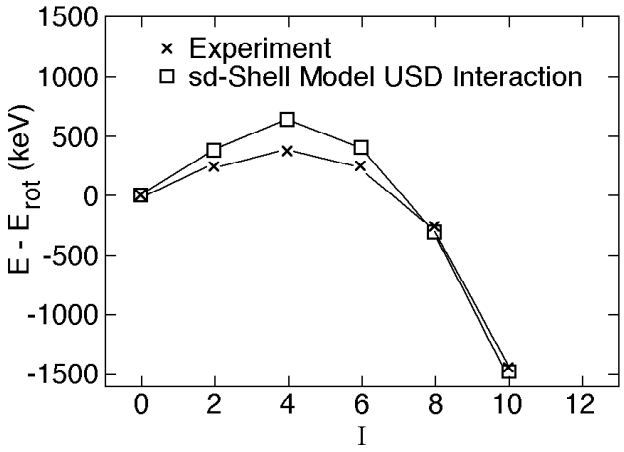

Fig. I-31. Excitation energies of the ground state band in ^{24}Mg, with a rotational reference $E_{rot}[MeV] = 0.187 * I(I + 1)$ subtracted. The experimental values are compared with the results of a sd-shell model calculation with the USD Hamiltonian discussed.

d.2. Search for Multi-Step Radiative Capture Decay of ^{24}Mg Following the ^{12}C + ^{12}C Reaction

(D. G. Jenkins,* C. J. Lister, M. P. Carpenter, R. V. F. Janssens, T. L. Khoo, F. G. Kondev, A. H. Wuosmaa, B. R. Fulton,† and M. Freer†)

In the seminal work of Sandorfi and Nathan,[1,2] the ^{12}C(^{12}C,γ) reaction was studied and high energy giant-resonance gamma ray decays to low-lying states in ^{24}Mg were observed using a large sodium iodide detector[1,2]. However, with such a set-up, it was not possible to look for multi-step decays through low-lying states in ^{24}Mg. It was therefore unclear whether multi-step decays existed or how preponderant they might be relative to the observed single step decays. Moreover, multi-step decays might populate exotic and non-yrast states not usually populated in heavy ion reactions; such states being selectively populated by their relation to the structure of the resonances. Thus, both the nature of the resonances, and exotic low-lying states may be probed by investigation of multi-step radiative capture.

Evidence for the existence of high spin resonances in the ^{12}C(^{12}C,γ) reaction comes from elastic and inelastic scattering, from direct gamma-ray yields and from studies of the inverse reaction; inelastic disintegration of ^{24}Mg into two ^{12}C nuclei. Spins of J = 4, 6, 8 and 10^+ were assigned to resonances in these breakup reactions by Fulton *et al.*[3] and Curtis *et al*[4]. Using the Gammasphere array, we tried to observe multi-step decay of the corresponding resonances in the ^{12}C(^{12}C,γ) reaction.

The measurement of high energy (> 5 MeV) γ-rays with a good experimental resolution is no easy task. A sodium iodide or barium fluoride detector gives good efficiency at the expense of resolution, while a germanium crystal has excellent resolution but very low efficiency at energies above 10 MeV. We explored a new mode of operating the Gammasphere array, where the energies recorded in the germanium crystals and the adjacent BGO shields are added up to provide "module" energy spectra. This mode of operation considerably increases the efficiency for high energy gamma rays at the expense of the optimal germanium resolution.

The ^{12}C + ^{12}C reaction was investigated at two energies, 16 and 22 MeV corresponding to the location of resonances assigned a spin of 4 and 8 respectively in break-up studies[3]. A ^{12}C beam from the ATLAS accelerator was incident on a 160 μg/cm2 ^{12}C target corresponding to an energy spread of 400 keV in the lab frame. At both beam energies, a clear end-point was seen in the sum energy spectrum corresponding closely to the maximum energy expected for the ^{12}C(^{12}C,γ) reaction (see Fig. I-32). The very large Q-value for the radiative capture process ensured a good separation from sum energy events from other reaction channels and from pile-up. By gating on the sum-energy region corresponding to radiative capture, it was possible to examine in detail the composition of the fully captured events. Approximately 100 events were separated in this manner for each beam energy, from the overwhelming background (> 10^7 events) from particle evaporation channels.

Our observations for the two cases are somewhat different. At the beam energy of 16 MeV, corresponding to a suggested spin 4 resonance, we observed decays consistent with this spin assignment. However, we do not see any evidence of feeding of the yrast 4^+ state but rather we observe decays principally to J = 2^+, 3^+, and 4^+ states in a rotational band assigned a label in the Nilsson scheme of K = 2 (see Fig. I-33). While these results are preliminary, they strongly hint at a good K quantum number for the resonance which explains the favorable decay to the K = 2 states. This supplies important information which is difficult to obtain by other methods, since only the energy and spin of the resonance may be obtained from reaction studies.

At the higher beam energy of 22 MeV, corresponding to a putative 8^+ resonance, the decay is much more compound-nuclear-like in character with a strong feeding of the yrast sequence from spin 6^+ down as well as many different states of diverse spin and parity. There does not appear to be a preference for any particular non-yrast states in the decay of the high spin resonance.

Clearly, there is much room for further work to develop on and understand our present results. In order to establish the relative cross-sections for the different decay patterns it is necessary to understand the efficiency of Gammasphere for these high energy gamma rays and detection using the "module" method. This was recently investigated during a short run at LBNL using the ^{11}B(p,γ) reaction at a proton energy of 7.5 MeV which produces gamma rays of 4.4,18.4 and

22.8 MeV. The analysis of this calibration data is in progress.

With the pattern of multi-step decay observed, it is possible to optimize the experimental conditions to obtain much better statistics. Obvious refinements to the experiment should substantially improve both the quantity and quality of the data. In addition, it is necessary to run both "on" and "off" resonance to confirm that these unusual decay events are truly resonant phenomena. A week-long Gammasphere run at LBNL is scheduled for March 2001.

In addition, substantial new information on states in ^{23}Na and ^{23}Mg, populated as a by-product of this experiment is being prepared for publication.

*University of Pennsylvania and Argonne National Laboratory, †University of Birmingham, United Kingdom

1A. M. Sandorfi, *Treatise on Heavy-Ion Science*, Vol. 2 Fusion and Quasi-Fusion Phenomena (ed. D. Allan Bromley).
2A. M. Nathan, A. M. Sandorfi and T. J. Bowles, Phys. Rev. C **24**, 932 (1981).
3B. R. Fulton, *et al*., Phys. Lett. **B267**, 325 (1991).
4N. Curtis, *et al*., Phys. Rev. C **51**, 1554 (1995).

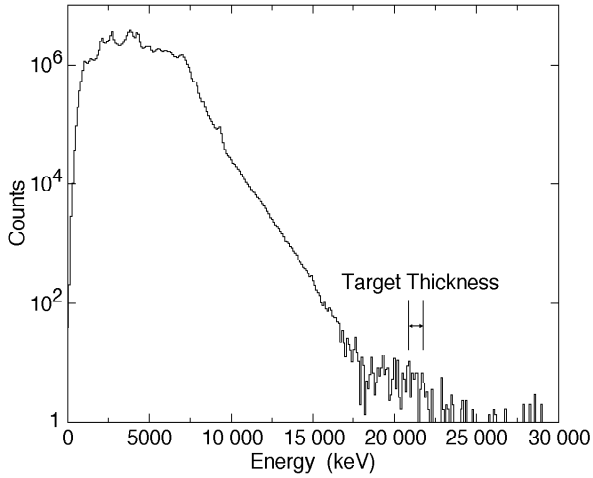

Fig. I-32. Sum energy spectrum from the 16 MeV data corresponding to a supposed spin of 4. The region correspondingto the target thickness is marked.

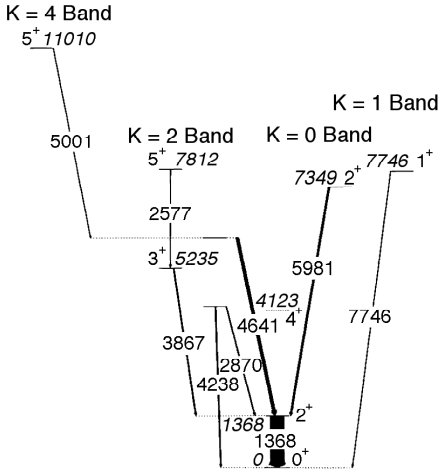

Fig. I-33. Decay scheme showing the states populated in the radiative capture decay of the 16 MeV resonance. The width of the arrows corresponds to the number of decays following the particular pathway. Not shown is the large energy gamma rays which decay from the resonance region to the low-lying states. The various rotational band members are labeled by their K quantum number with the Nilsson scheme. The unpopulated yrast 4+ state is shown as a dotted line.

d.3. Lifetime of the Superdeformed Band in the N = Z Nucleus ^{36}Ar

(R. V. F. Janssens, M. P. Carpenter, D. Seweryniak, C. E. Svensson,* A. O. Macchiavelli,* A. Juodagalvis,† A. Poves,‡ I. Ragnarsson,† S. Aberg,† D. E. Appelbe,§ R. A. E. Austin,§ G. C. Ball,¶ E. Caurier,|| R. M. Clark,* M. Cromaz,* M. A. Deleplanque,* R. M. Diamond,* P. Fallon,* G. J. Lane,* I. Y. Lee,* F. Nowacki,|| D. G. Sarantites,** F. S. Stephens,* K. Vetter,* and D. Ward*)

Last year we reported on a superdeformed band in the N = Z nucleus ^{36}Ar identified with the Gammasphere spectrometer and the microball array. The band was firmly linked to known low-spin states in this nucleus and was traced to its presumed termination (spin 16). Deformed mean field and spherical shell model calculations lead to a configuration assignment in which four fp-shell orbitals are occupied. This band involves the cross-shell correlations typical of rotational motion in heavier nuclei, while the number of active particles remains sufficiently small to be confronted with the spherical shell model. The latter calculations support the $(fp)^4$ assignment, but suggest that the entire sd-shell is also essential for the full description of this band. Hence, ^{36}Ar provides an ideal case to investigate the microscopic origin of collective rotation in nuclei. A paper reporting these results was recently published.[1]

In a second ATLAS experiment, lifetimes have now been measured for all the states in the superdeformed band using the DSAM technique. The reaction ^{24}Mg(^{20}Ne,2α)^{36}Ar at 80 MeV was used in conjunction with Gammasphere and microball. A large quadrupole deformation ($\beta_2 = 0.46 \pm 0.03$) is confirmed at the bottom of the band with a considerable decrease in collectivity as the high-spin band termination is approached. This can be seen in Fig. I-34. Detailed comparisons of the experimental B(E2) values with the results of cranked Nilsson-Strutinsky and large scale spherical shell model calculations indicate the need for a more refined treatment of transition matrix elements close to termination in the former, and the inclusion of the complete sd-pf model space in the latter description of this highly-collective rotational band. A paper reporting these results was recently submitted for publication as a Rapid Communication in the Physical Review.

*Lawrence Berkeley National Laboratory, †Lund Institute of Technology, Sweden, ‡University of Madrid, Spain, §McMaster University, Hamilton, Canada, ¶TRIUMF, Vancouver, Canada, ||IReS, Strasbourg, France, **Washington University

[1] C. E. Svensson *et al*., Phys. Rev. Lett. **85**, 2693 (2000).

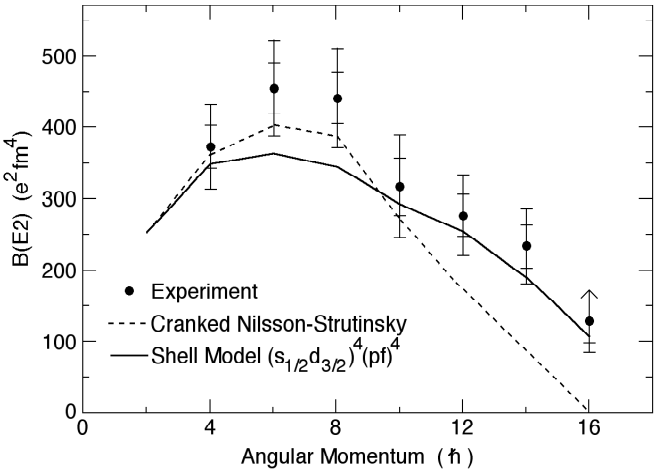

Fig. I-34. B(E2) values for the superdeformed band in ^{36}Ar compared with the results of cranked Strutinsky (dashed line) and shell model (solid line) calculations. The inner error bars represent the statistical uncertainties, while the outer error bars show the effects of systematic uncertainties associated with the stopping powers inherent to DSAM measurements.

d.4. Band Structure of ^{68}Ge

(M. P. Carpenter, R. V. F. Janssens, D. Seweryniak, D. Ward,* C. E. Svensson,*† I. Ragnarsson,‡ C. Baktash,§ M. A. Bentley,¶ J. A. Cameron,† R. M. Clark,* M. Cromaz,* M. A. Deleplanque,* M. Devlin,|| R. M. Diamond,* P. Fallon,* S. Flibotte,† A. Galindo-Uribarri,§ D. S. Haslip,† T. Lampman,† G. J. Lane,* I. Y. Lee,* F. Lerma,|| A. O. Macchiavelli,* S. D. Paul,§ D. Radford,§ D. Rudolph,‡ D. G. Sarantites,|| B. Schaly,† F. S. Stephens,* O. Thelen,** K. Vetter,* J. C. Waddington,† J. N. Wilson,|| and C. Y. Yu§)

The nucleus ^{68}Ge was studied by gamma-ray spectroscopy following its population at high spin in the reaction ^{40}Ca(^{32}S,4p)^{68}Ge. The ^{32}S beam was delivered by ATLAS. The reaction channel was selected with the Microball array and gamma rays were detected with the Gammasphere array. Events were recorded when a trigger on fourfold (or higher) clean γ-coincidences in the Compton suppressed array was issued. Approximately 1.7×10^9 events were recorded to tape.

The deduced level structure of ^{68}Ge is very complex, reflecting the many different, and presumably mixed, modes of excitation in this nucleus. Nevertheless, there appears to be some simplifications in the spin range above 18 h where we identified a superdeformed band and several terminating bands. In cranked Nilsson-Strutinsky calculations, four energetically favored high-spin configurations are identified within the valance space outside the ^{56}Ni core. They involve various numbers of proton and neutron $g_{9/2}$ excitations and give rise to bands terminating at 23$^-$, 25$^+$, 26$^+$, and 28$^-$ corresponding exactly with the highest spins of the experimentally observed bands. The identified superdeformed band is populated at ~0.2% of the ^{68}Ge channel intensity. It was assigned a configuration in which the ^{56}Ni core was broken and two protons were identified from the $f_{7/2}$ orbital.

A paper reporting the results of this work was published recently in Physical Review C[1].

*Lawrence Berkeley National Laboratory, †McMaster University, Hamilton, Ontario, ‡Lund University, Sweden, §Oak Ridge National Laboratory, ¶Staffordshire University, Stoke-on-Trent, United Kingdom, ||Washington University, **University of Cologne, Germany

[1] D. Ward *et al.*, Phys. Rev. C **63**, 014301 (2001).

d.5. Stability of Oblate Shapes in the N = Z + 1 Nucleus ^{69}Se

(D. G. Jenkins,* D. P. Balamuth,† M. P. Carpenter, C. J. Lister, S. M. Fischer,‡ R. M. Clark,§ A. O. Macchiavelli,§ P. Fallon,§ C. E. Svensson,§ N. S. Kelsall,¶ and R. Wadsworth¶)

The observation of oblate shapes in nuclei is relatively rare despite naive expectations which would suggest equal probabilities for the occurrence of oblate and prolate shapes based on the frequency of deformation-stabilizing down-sloping high-j orbitals for both shapes.[1] The reasons for the suppression of oblate deformation is subtle and lies in higher order effects both in liquid drop terms and residual interactions. An oblate spheroid rotating about an axis perpendicular to the symmetry axis has the lowest moment of inertia of all possible shapes. The consequence of this is that oblate rotational bands are quickly supplanted by competing configurations which have larger moments of inertia, so oblate shapes are experimentally difficult to observe.

Long standing predictions of a stable oblate minimum for N = Z = 34 were recently confirmed by the observation of an oblate ground state band in ^{68}Se.[2] This configuration competes successfully with a prolate rotational band and the crossing does not happen till J ~ 8 h. The ground state band exhibits no back-bending in the range in which it is observed; an observation fully consistent with an oblate assignment. This successful study of ^{68}Se was partly prompted by earlier studies of ^{69}Se where the measurement of a positive value for the multipole mixing ratio of an M1/E2 transition inferred an oblate configuration.[3,4] We have come full circle and revisited ^{69}Se as well as ^{67}As, in a study of oblate bands and their competition with higher moment-of-inertia configurations at high spin.

Information on states in ^{69}Se was derived from two reactions. In the first, a ^{63}Ar beam accelerated to 145 MeV by ATLAS was incident on a thick ^{40}Ca target. Recoiling nuclei were stopped 1-mm downstream of this target in a 15-mg/cm^2 thick gold foil. The second source of information on ^{69}Se used the ^{40}Ca(^{32}S,2pn) reaction employing a 100-MeV beam of ^{32}S incident on the same ^{40}Ca target as before but with the stopper foil removed. In both cases, the resulting gamma decay was detected by the Gammasphere array of 80 HPGe detectors with channel selection provided by an array of 30 NE213 neutron detectors and the Microball array of 95 CsI detectors.

The ^{69}Se level scheme was enlarged considerably and the $g_{9/2}$ band was extended up to a tentative spin of $(41/2^+)$ (see Fig. I-35).

Clearly the ^{69}Se level scheme is rather complicated and, with the exception of the $g_{9/2}$ band, the intensity is spread over many irregular levels. Above spin $17/2^+$, the $g_{9/2}$ band appears to change character. Below this level, the band is strongly-coupled which is indicative of an oblate deformation, since only in the case where K is a good quantum number and the valence neutron occupies a high-K (9/2) orbit can the strong coupling be accounted for in this nucleus. In addition, we extracted positive mixing ratios for the mixed dipole transitions which are further evidence for oblate deformation. Above spin $17/2^+$ the band is decoupled and no signature partner can be found despite a careful search. Two backbendings are observed in this decoupled portion, the first at a rotational frequency of around 0.60 MeV/h and a second at around 0.85 MeV/h. Cranking calculations assuming an oblate deformation of $\varepsilon_2 = -0.3$ indicate that no alignment processes take place for either protons or neutrons until very high rotational frequencies (> 1 MeV h) are reached. It is necessary to invoke a prolate deformation of $\beta_2 = 0.3$ to account for the observed backbending in the high spin portion of the band. This points to a crossing of the oblate band by a prolate configuration.

We conclude that the oblate minimum is not as deep in ^{69}Se as it is in its self-conjugate core ^{68}Se. This is indicated by the rapid crossing of an oblate rotational band by prolate configurations which dominate the high spin yrast-line. This work was submitted for publication.

---

*University of Pennsylvania and Argonne National Laboratory, †University of Pennsylvania, ‡DePaul University, §Lawrence Berkeley National Laboratory ¶University of York, United Kingdom

1A. Bohr and B. R. Mottelson, Nuclear Structure Vol. II: Nuclear Deformations W. A. Benjamin, New York (1975).

2S. M. Fischer, D. P. Balamuth, P. A. Hausladen, C. J. Lister, M. P. Carpenter, D. Seweryniak, and J. Schwartz, Phys. Rev. Lett. **84**, 4064 (2000).

3M. Wiosna, J. Busch, J. Eberth, M. Liebchen, T. Mylaeus, N. Schmal, R. Sefzig, S. Skoda, and W. Teichert, Phys. Lett. **B200**, 255 (1988).

4J. W. Arrison, D. P. Balamuth, T. Chapuran, D. G. Popescu, J. Görres, and U. J. Hüttmeier, Phys. Rev. C **40**, 2010 (1989).

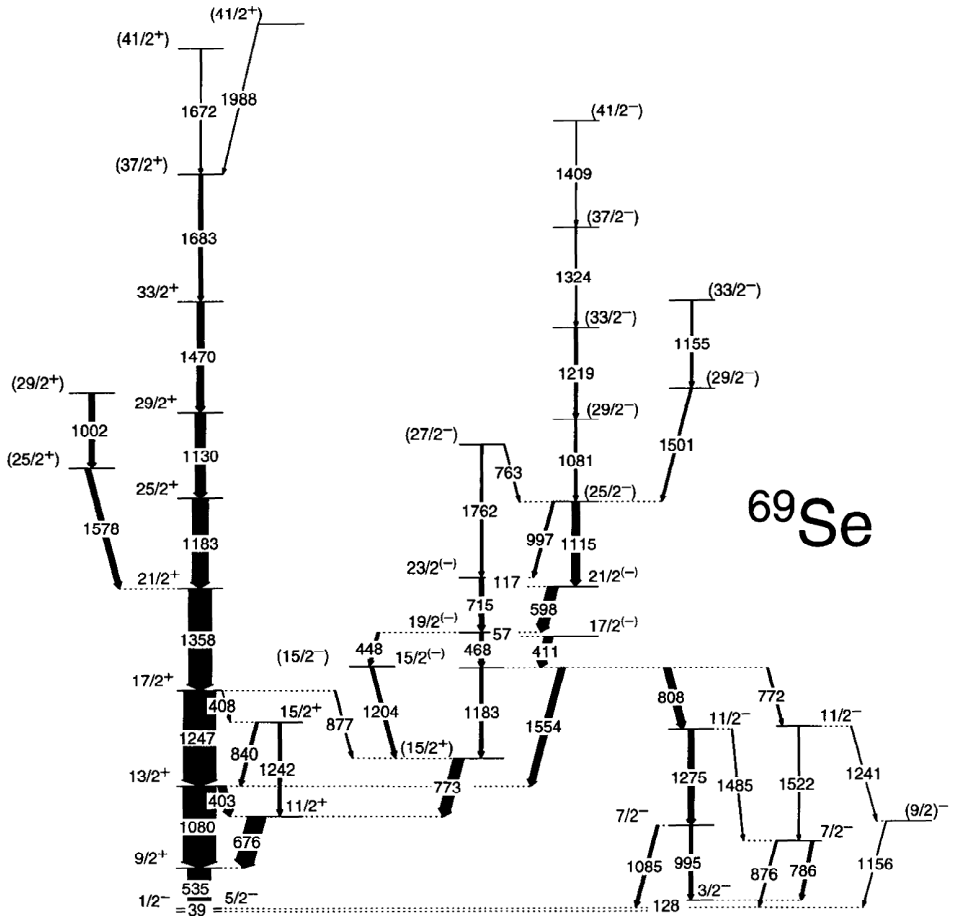

Fig. I-35. Partial level scheme for ^{69}Se. The width of the arrows is proportional to the intensity of the transitions.

d.6. Superdeformation in ^{91}Tc

(R. V. F. Janssens, M. P. Carpenter, F. G. Kondev, T. Lauritsen, C. J. Lister, D. Seweryniak, I. Wiedenhöver, E. Ideguchi,* B. Cederwall,* R. Wyss,* T. Back,* K. Lagergren,* A. Johnson,* W. Klamra,* J. Cederkal,* M. Devlin,† J. Elson,† D. R. Lafosse,† F. Lerma,† D. G. Sarantites,† V. Tomov,† M. Haussman,‡ A. Jungclaus,‡ D. R. Napoli,§ R. M. Clark,¶ P. Fallon,¶ I. Y. Lee,¶ A. O. Macchiavelli,¶ and R. W. MacLeod¶)

In an experiment performed with Gammasphere and microball at ATLAS, a high-spin rotational band with 11 gamma-ray transitions was observed in ^{91}Tc. The dynamical moment of inertia as well as the transition quadrupole moment of 8^{+19}_{-14} eb measured for this band show characteristics of a superdeformed band. However, the associated shape is more elongated than in the neighboring A = 80-90 superdeformed nuclei. Theoretical interpretations of the band within the cranked Strutinsky approach based on different Woods-Saxon potential parameterizations were carried out. Even though an unambiguous configuration assignment proved difficult, all calculations indicate a larger deformation and at least three additional high-N intruder orbitals occupied compared to the lighter superdeformed nuclei. A paper presenting these results was recently published.[1]

*Royal Institute of Technology , Stockholm, Sweden, †Washington University, ‡University of Göttingen, Germany, §Legnaro National Laboratory, Italy, ¶Lawrence Berkeley National Laboratory

1E. Ideguchi *et al.*, Phys. Lett. **B492**, 245 (2000).

d.7. ^{98}Tc, BIC and the Lifetime of the 21.8-keV Level

(I. Ahmad, K. E. Rehm, J. F. Smith,* J. S. Lilley,* W. R. Phillips,* and A. Garcia†)

The 21.8-keV level in ^{98}Tc is of interest because it is a candidate for studies of bound internal conversion (BIC)[1] in which a nuclear level decays partly by exciting a K shell electron to bound atomic states. The BIC process is the inverse of NEET,[2] nuclear excitation by electronic transfer, which recently received renewed attention. The 21.8-keV level in the neutral atom decays predominantly via internal conversion in the K shell. When the electrons are stripped off the Z = 43 Tc atom to produce charge state q = 20, which has Z-q = 23 remaining electrons, the binding energy of a K shell electron is predicted by the code GRASP (which is accurate to better than 100 eV) to exceed 21.8 keV. K conversion of the nuclear state with emission of the electron in the continuum is no longer possible after charge state 19. Measurements of lifetime changes in charge states above 19 will give BIC decay probabilities.

Levels in ^{98}Tc were excited in the ^{98}Mo(p,n)^{98}Tc reaction by 5 MeV protons from the FN tandem accelerator of the University of Notre Dame. The ^{98}Mo target was 3 mg/cm^2 thick and had the isotopic purity of 98%. The recoiling ^{98}Tc atoms stopped in the target. In one experiment a Si(Li) detector and a low energy photon spectrometer (LEPS) were used to measure the γ and x rays and level lifetimes. In another experiment a LEPS and a thin BaF_2 detector were used. The low energy γ ray spectrum measured with the LEPS spectrometer and in coincidence with low energy γ rays and x rays is displayed in Fig. I-36. From the analysis of the data set a half-life of 2.4(6) ns was obtained for the 21.8-keV state in ^{98}Tc. The results will be published in Phys. Rev. C.

*University of Manchester, United Kingdom, †University of Notre Dame

1T. Carreyer *et al*., Phys. Rev. C **62**, 024311 (2000).

2S. Kishimoto *et al*., Phys. Rev. Lett. **85**, 1831 (2000).

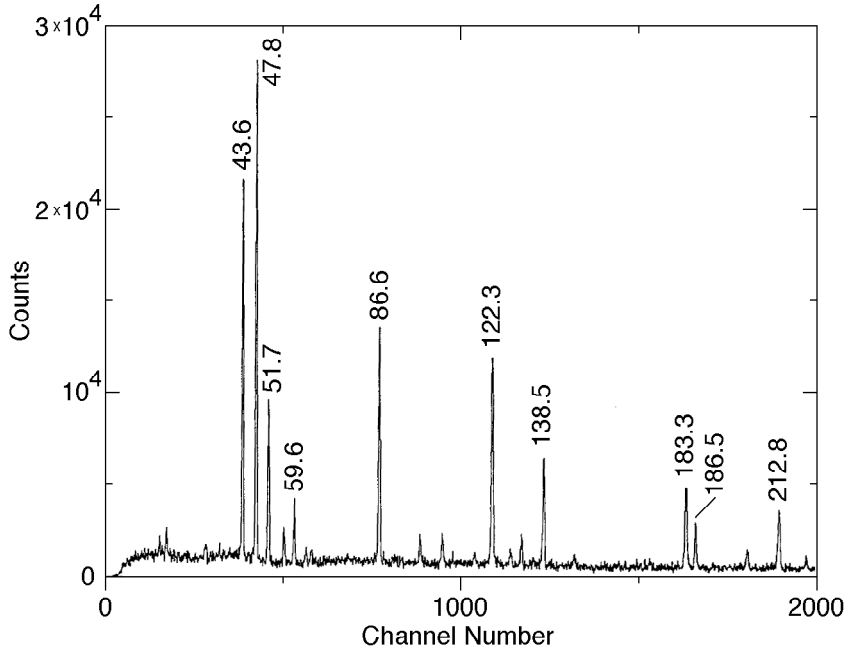

Fig. I-36. Gamma ray spectrum of ^{98}Tc measured with a LEPS spectrometer in coincidence with x rays and low energy γ rays in a Si(Li) spectrometer.

d.8. High-Spin States in $Z \approx 59$, $A \approx 130$ Nuclei

(M. P. Carpenter, R. V. F. Janssens, D. Seweryniak, D. J. Hartley,* O. Zeidan,* H. Park,* L. L. Riedinger,* M. Danchev,* W. Reviol,* A. Galindo-Uribarri,† C. J. Gross,† C. Baktash,† M. Lipoglavsek,† S. D. Paul,† D. C. Radford,† C.-H. Yu,† D. G. Sarantites,‡ and M. Devlin‡)

At one time, gamma-ray spectroscopy in the very neutron-deficient nuclei of the mass 130 region was very difficult due to the dominant charged-particle evaporation from the compound nucleus which produced numerous less exotic isotopes. However, with the Washington University Microball in conjunction with Gammasphere, this channel fragmentation problem turned into an asset. By correlating γ rays detected in Gammasphere with protons and alphas detected in the Microball, many new transitions may be uniquely associated with charged-particle emission channels. Thus, as many as twenty different nuclei may be studied from one experiment.

In an investigation of nuclei approaching the proton drip line, the reaction ^{40}Ca + ^{92}Mo was used at a beam energy of 184 MeV. The beam was provided by the ATLAS facility at ANL and Gammasphere with the Microball was employed to detect the emitted γ rays and charged particles. In addition, the same reaction was used at ORNL with the Clarion Ge array, HyBall CsI array, and the Recoil Mass Spectrometer. More than fifteen nuclei were observed ranging in proton number from Z = 55 to 60.

A new sequence of transitions was correlated with a mass of 126 from the ORNL experiment and with the emission of an alpha and a proton from the ANL experiment. This led to the first conclusive evidence of excited states in $^{126}_{59}$Pr, which is now the lightest known odd-odd Pr nucleus. A second structure observed in the ANL data, but not in the ORNL data, was also tentatively assigned to ^{126}Pr. The former band was assigned the $\pi_{h11/2}\nu h_{11/2}$ configuration and the phenomenon of signature inversion[1] was observed. Systematics in this signature inversion were studied in $_{55}$Cs, $_{57}$La, and Pr odd-odd nuclei. Surprisingly, opposite trends in the amount of energy splitting between the two signatures was found between the Cs and Pr nuclei. These opposing systematics pose a substantial challenge for theorists to reproduce. A manuscript on this subject was accepted by Physical Review C as a Rapid Communication.

Preliminary reports[2] of a sequence in $^{129}_{60}$Nd were confirmed and three new structures were established through the combination of the two experiments. An adiabatic crossing in one of the positive-parity bands is reminiscent of the highly deformed $\nu i_{13/2}$ band crossing a normal deformed structure in ^{131}Nd (Ref. 3). Therefore, there is evidence of this deformation driving orbital at a relatively low neutron Fermi surface of N = 69 in ^{129}Nd. The ground-state band of ^{128}Nd was also extended to higher spin and four side bands were observed for the first time.

Over 150 new transitions were added to the level schemes of ^{128,129}Pr. Highly deformed structures based upon a hole in the $\pi g_{9/2}$ orbital are observed in both nuclei. These bands are nearly identical at low spins in ^{128,129,130}Pr, but the identical transitions depopulate states that differ by 2 h in ^{128}Pr and ^{130}Pr (Ref. 4). Additionally, a similar adiabatic crossing is observed in ^{128}Pr as that seen in ^{129,131}Nd, indicating the possible presence of the highly deformed $\nu i_{13/2}$ orbital. High-K bands, based upon three- and four quasiparticle configurations, were also observed in ^{129}Pr and ^{128}Pr, respectively.

Significant improvement in the level schemes of ^{123}La and ^{126}Ce was established from this experiment. Three graduate students will incorporate data from this fruitful experiment as part of their theses and several papers shall follow as our analysis continues.

---

*University of Tennessee, †Oak Ridge National Laboratory, ‡Washington University

1R. Bengtsson *et al*., Nucl. Phys. **A415**, 189 (1984).
2D. C. B. Watson *et al*., Daresbury Lab., Annual Report, 1986-87, Appendix, p. 31 (1987).
3D. J. Hartley *et al*., Phys. Rev. C **60**, 041301(R) (1999).
4B. H. Smith *et al*., Phys. Lett. **B443**, 89 (1998).

d.9. Experimental Determination of the Excitation Energy, Spin and Parity of the Yrast Superdeformed Band in ^{152}Dy from the 4010 keV One-step Linking Transition

(T. Lauritsen,* M. P. Carpenter,* P. Fallon,† B. Herskind,‡ R. V. F. Janssens,* D. Jenkins,* T. L. Khoo,* F. G. Kondev,* A. Lopez-Martens,§ A. O. Macchiavelli,† D. Ward,† I. Ahmad,* R. Clark,† M. Cromaz,† T. Døssing,‡ J. P. Greene,* F. Hannachi,§ A. M. Heinz,* A. Korichi,§ G. Lane,† C. Lister,* and R. C. Vondrasek*)

A 4010 keV one-step direct linking transition connects the yrast superdeformed level fed by a 693 keV transition to the J = 27 yrast state in ^{152}Dy. This is the first one-step linking transition observed in the A = 150 superdeformed mass region. The excitation energy of the de-exciting superdeformed state is thus determined as 11,891 keV. The linking transition is either of stretched or anti-stretched E1 character, hence, the spin of the feeding state is 28^+ or 26^+. The average spin removed by all decay gamma rays favors the 26^+ assignment, but the 28^+ assignment cannot be ruled out. The 4010 keV transition has a strength of 7×10^{-7} W.u. and carries only 0.9% of the intensity of the superdeformed band. Thus, eighteen years after it was discovered, the first discrete superdeformed band is finally linked to its yrast states.

The 4010 keV linking transition in ^{152}Dy, and hints of others, was first observed in a GS experiment performed at Argonne National Laboratory. The SD band in ^{152}Dy was populated with the reaction ^{76}Ge(^{80}Se,4n)^{152}Dy. Due to the weak intensity of the observed linking transitions, another much longer experiment (12 days) was performed with GS, after it had moved back to Lawrence Berkeley National Laboratory. This time the ^{152}Dy SD band was populated with the reaction ^{108}Pd(^{48}Ca,4n)^{152}Dy. Beams were delivered by the 88" Cyclotron at an energy of 191 MeV (at mid-target). The target consisted of a stack of two 0.4 mg/cm^2 self supporting ^{108}Pd foils.

In order to tag on the gamma rays emitted under the 60 nsec isomer in the recoiling ^{152}Dy residues, a Pb stopper foil was placed in the downstream beam-line between the forward BGO Compton shield detectors. The so-called tagging efficiency was estimated to be ~ 70%. A total of 4.6×10^9 (after prompt time requirements) triple- or higher-fold coincidence events were collected. When requiring the observation of delayed gamma rays in the forward BGO detectors 1.6×10^9 events remained, almost exclusively corresponding to the ^{152}Dy reaction channel.

Figure I-37 shows high energy part of the spectrum obtained from placing pairwise coincidence gates on transitions in the yrast SD band in ^{152}Dy after the delayed isomer tag was applied. Several candidates for decay-out transitions are clearly seen. In particular gamma rays at 2712 and 4010 keV are prominent. The spectrum obtained from setting pairwise gates on SD lines and the 4010 keV transition is presented in Fig. I-38. It is clearly seen that the 647 and 602 SD lines (see Fig. I-39) are not in coincidence with the 4010 keV gamma ray whereas the 693 keV and higher SD lines are. This unambiguously determines that the 4010 keV transition originates from the SD level fed by the 693 keV line. Of the yrast lines in the spectrum the 221 and 541 keV gamma rays are very strong -- whereas there is no indication of a 967 keV transition or any extra strength on the low energy side of the 969 keV SD transition. Thus, the 4010 keV gamma ray clearly feeds into the 27-normal state. The lack of any new, unassigned lines in the very clean spectrum in Fig. I-37 strongly suggests that the feeding is direct and not through any intermediate level above the yrast line. This establishes the excitation energy of the SD level fed by the 693 SD line to be 11,891 keV.

To establish the spin of the SD level fed by the 693 SD line an angular distribution analysis of the 4010 keV one-step linking transition was performed. The result is shown in Fig. I-39. The 4010 keV one-step transition as well as other decay gamma rays are shown in the level scheme in Fig. I-40.

*Argonne National Laboratory, †Lawrence Berkeley National Laboratory, ‡The Niels Bohr Institute, Denmark, §CSNSM., IN2P3-CNRS, Orsay, France

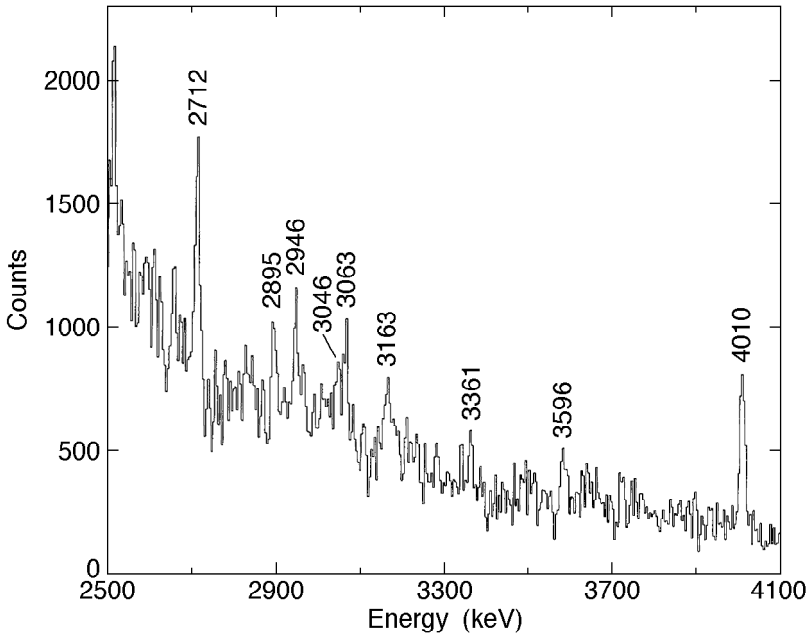

Fig. I-37. The summed spectrum obtained from placing pairwise coincidence gates on transitions in the yrast SD band in ^{152}Dy. The data are the sum from both the ANL and LBNL data sets and are shown with a dispersion of 4 keV/channel. The data from ANL used triple gating and the LBNL data used double gating with a tag on the isomer. This spectrum is raw data, i.e., it has not been corrected for efficiency nor unfolded. A number of candidates for DO gamma rays are seen -- in particular the 2712 and 4010 keV transitions. A number of other weaker candidates (many clustered near 3 MeV) are labeled on the plot as well. The 4010 keV transitions has a total of 2400 counts in the raw spectrum. No transitions above 4010 keV are observed.

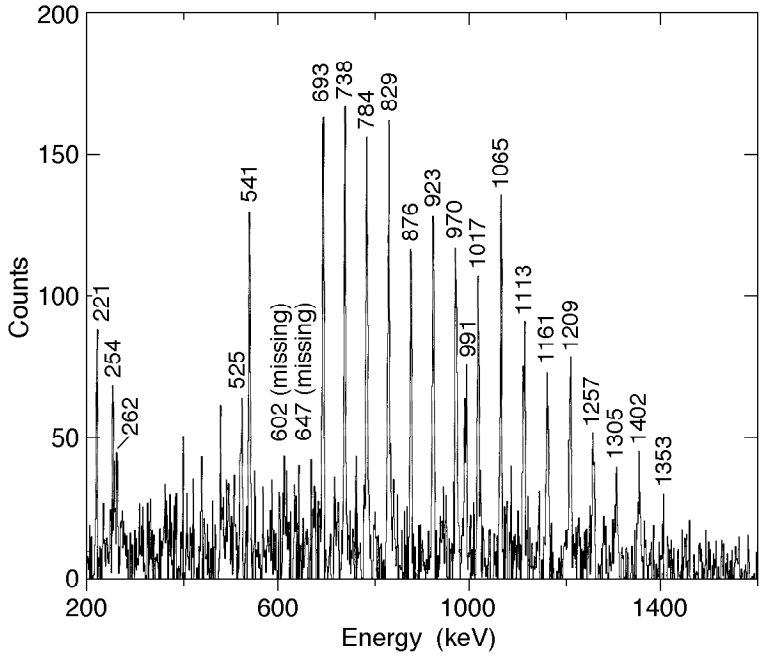

Fig. I-38. The spectrum obtained from setting pairwise gates on an SD line and the 4010 keV transition. A delayed isomer tag was required as well.

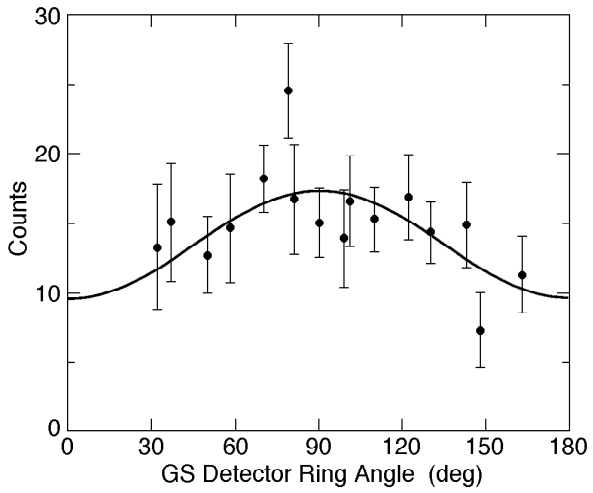

Fig. I-39. Yield of the 4010 keV one-step DO link as a function of the angle of the detector ring in GS. There were no detectors in the 17 deg. forward ring. The fitted angular distribution coefficients are: A_2 = -0.35(12) and A_4 = -0.02(16).

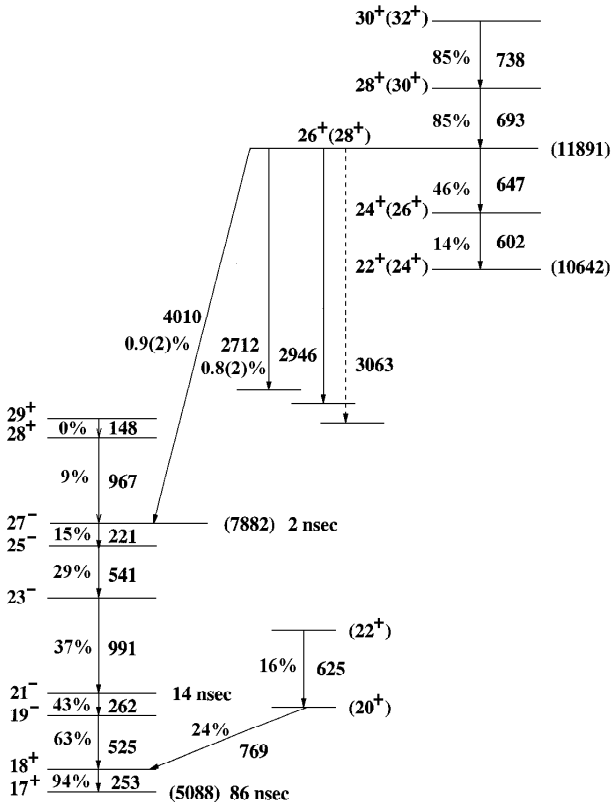

Fig. I-40. Partial level scheme showing the lowest part of the yrast SD band and a selected set of normal lines above the 60 nsec isomer in ^{152}Dy. Only the 4010 keV transition links directly to the 27$^-$ state in the normal level scheme. For the other primary transitions at 2712, 2947 and 3066 keV the complete decay patch is not observed. After the intermediate levels indicated, the decay becomes too fragmented to follow. The decay gamma rays from this point on are embedded into the QC in coincidence with the SD band. The levels from which the 769 and 624 keV transitions emanate collect a significant fraction of the flux from the decay of the SD band. This flux bypass the isomer at 21$^-$.

d.10. First Evidence for Triaxial Superdeformation in ^{168}Hf

(R. V. F. Janssens, M. P. Carpenter, T. L. Khoo, F. Kondev, T. Lauritsen, C. J. Lister, S. Siem, I. Wiedenhöver, H. Amro,* P. G. Varmette,* W. C. Ma,* B. Herskind,† G. B. Hagemann,† G. Sletten,†, M. Bergstrom,† A. Bracco,‡ J. Domscheit,§ S. Frattini,‡ D. J. Hartley,¶ H. Hubel,§ B. Million,‡ S. Odegaerd,† R. B. Piercey,* L. L. Riedinger,¶ K. A. Schmidt,§ J. N. Wilson,† and J. A. Winger*)

In experiments with Gammasphere at ATLAS, three superdeformed (SD) bands were found in ^{168}Hf. Lifetime measurements revealed a large quadrupole moment, Q ~ 11.4 eb, for the strongest superdeformed band. This value is about twice as large as that for the normal deformed structures in this nucleus. Theoretical calculations using the "ultimate cranker" code predict high-spin SD minima with stable triaxial deformations of gamma ~ +20 degrees and gamma ~ -15 degrees. The measured Q value suggests that the strongest superdeformed band corresponds to a deformation with a positive gamma value. This constitutes the first evidence for triaxial superdeformation in an even proton system. The population intensities of the bands indicate a far greater role for the proton shell gap and a different trend in the evolution with mass of the neutron shell gap as compared with theoretical calculations. A paper summarizing these results was submitted for publication.

*Mississippi State University, †Niels Bohr Institute, Copenhagen, Denmark, ‡University of Milano, Italy, §University of Bonn, Germany, ¶University of Tennessee

d.11. First Observation of Excited Structure in Neutron-Deficient ^{179}Hg: Evidence for Multiple Shape Coexistence

(F. G. Kondev, I. Ahmad, H. Amro,* J. Caggiano, M. P. Carpenter, C. N. Davids, A. Heinz, R. V. F. Janssens, T. L. Khoo, T. Lauritsen, C. J. Lister, J. Ressler,§ D. Seweryniak,§ S. Siem,** A. A. Sonzogni, I. Wiedenhöver, B. Herskind,† W. C. Ma,‡ W. Reviol,¶ L. L. Riedinger,|| and P. G. Varmette‡)

Coexistence between different shapes in a single nucleus is a general phenomenon of nuclei located near shell gaps. This occurrence is usually associated with the interplay between the occupation of specific intruder orbitals and the stabilizing role played by the shell closures. Experimental investigations of the development of shape coexistence through and beyond the mid-shell and the interaction between coexisting configurations play an important role in understanding the structure of the nucleus at the extremes in N/Z ratio, excitation energy and angular momentum. They also provide opportunities to test the robustness of various theoretical models in predicting the single-particle states near the proton-drip line and in elucidating their effect on the onset of new shell closures.

Excited states in ^{179}Hg were populated in the 1*n* channel of the symmetric ^{90}Zr + ^{90}Zr reaction. The beam with energies of 369 and 380 MeV was delivered by the ATLAS superconducting linear accelerator at Argonne National Laboratory. A self-supporting, ~500 μg/cm2 thick target, enriched up to 97.65% with ^{90}Zr, was used. Because of the large and negative Q value of -157.3 MeV the compound nucleus was populated at relatively low excitation energies of E* = 23.5 and 29.0 MeV (assuming production in the middle of the target) which minimizes the fission and the charged particle emission competitions. Prompt γ rays were detected with the Gammasphere array in conjunction with the recoil-decay tagging technique, following mass selection.

The striking feature of the ^{179}Hg level scheme is the competition between structures associated with *three* different minima: weakly prolate (triaxial), oblate and prolate. By combining the simplicity of the α-decay properties of ^{179}Hg and of its daughter (^{175}Pt), and grand-daughter (^{171}Os) nuclei with the complexity of the γ-ray spectroscopic information we established the spin and parity of the ^{179}Hg ground state as $I\pi = 7/2^-$ and assigned it the mixed $f_{7/2}/h_{9/2}$ configuration which originates from a weakly prolate (*triaxial*) shape. This observation is supported by complementary total Routhian surface (TRS) calculations which predict β_2 = 0.112 and $\gamma \sim 37°$ for the above configuration. Three *prolate* collective bands were observed to compete for

favored yrast status at higher excitation energies. Sample γ-ray coincidence spectra are shown in Fig. I-41. The bands are assigned the 5/2-[512], 1/2-[521] and 7/2+[633] Nilsson configurations on the basis of the measured in-band properties such as branching ratios and alignments, as well as on considerations about which orbitals are expected near the neutron Fermi surface. Similarities with known structures in neighboring odd-mass Hg and Pt nuclei were also helpful. A high-spin 13/2+ isomer, analogous to those seen in the heavier Hg isotopes was also observed and assigned the *oblate* 13/2+[606] neutron configuration.

*Argonne National Laboratory and Mississippi State University, †The Niels Bohr Institute, Copenhagen, Denmark, ‡Mississippi State University, §Argonne National Laboratory and University of Maryland, ¶University of Tennessee-Knoxville and Washington University-St. Louis, ||Washington University-St. Louis, **Argonne National Laboratory and University of Oslo, Norway, ††University of Oslo, Norway

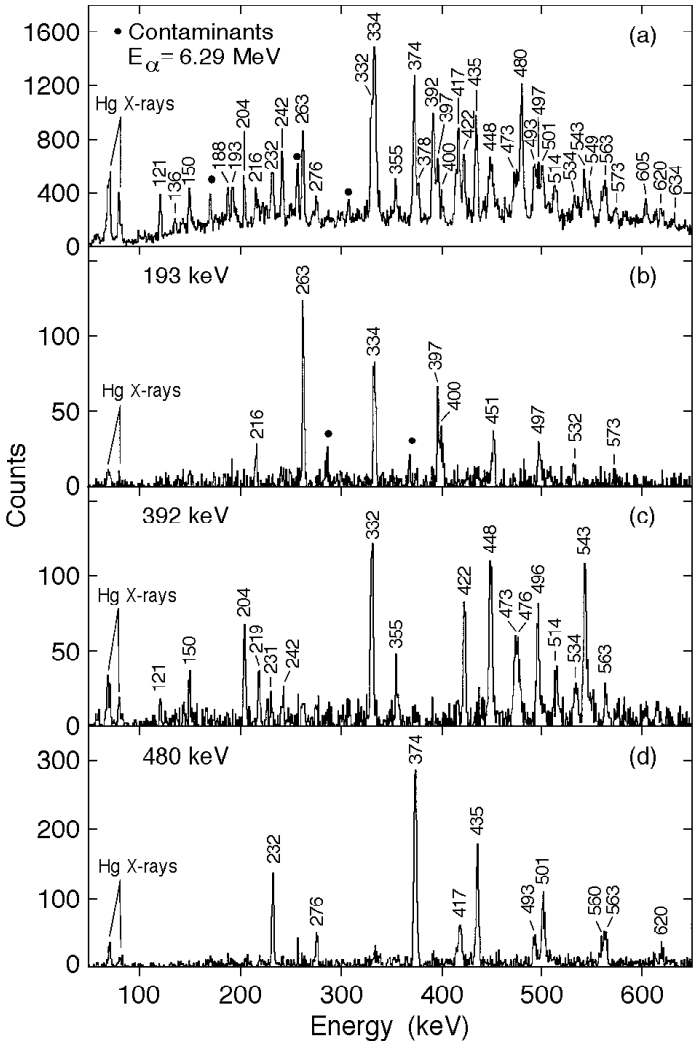

Fig. I-41. (a) Spectrum of γ rays correlated with the ^{179}Hg α line of E_α = 6.29 MeV. (b), (c) and (d) Sample background-subtracted γ-ray coincidence spectra from the recoil-γ-γ matrix.

d.12. First Observation of Rotational Band in Neutron-Rich ^{180}Lu

(F. G. Kondev, I. Ahmad, M. P. Carpenter, R. V. F. Janssens, T. L. Khoo, C. J. Lister, D. Seweryniak, I. Wiedenhöver, P. Chowdhury,* I. Shestakova,* R. D'Alarcao,* C. Wheldon,† P. M. Walker,† C. J. Pearson,† Zs. Podolyak,† and D. M. Cullen‡)

The rare-earth nuclei around A ~ 180 have proton and neutron orbitals lying close to the Fermi surface with large angular momentum projections, on the nuclear symmetry axis. When combined with the pronounced mid-shell prolate deformations in these nuclei, the total angular momentum projection on the symmetry axis, K, becomes an approximately conserved quantity. Metastable or isomeric states arise because they decay by transitions that have to effect a large change in the K quantum number and are thus hindered. However, the study of these states has predominantly been restricted to the neutron-deficient side of the β-stability line. Although predictions exist[1] for long-lived high-K states in neutron-rich nuclei, these cannot be populated using fusion-evaporation reactions with stable beam and target combinations.

Lutetium isotopes (Z = 71) have some of the largest quadrupole deformations in the region and some of the longest lived K-isomers observed so far. They also exhibit unusual phenomena including K-driven β-decays. The longest-lived lutetium isomers are in the neutron-rich isotopes. For example, a 160 day three-quasiparticle isomer was identified in ^{177}Lu. Indeed, ^{177}Lu is the most neutron-rich isotope that can be populated in fusion-evaporation reactions and even with light-ion projectiles (^{7}Li and ^{4}He) the population takes place through the weak α2n and p2n channels. To study more neutron-rich isotopes, it is necessary to use another method. Historically, transfer reactions with tritium beams were used to identify low-spin states in ^{178}Lu and ^{179}Lu. However, this technique is generally restricted to in-beam spectroscopy of low-lying states. Several recent studies using deep-inelastic reactions with heavy-ion projectiles proved very successful in populating high-K isomers in neutron-rich nuclei.

The ATLAS accelerator facility at Argonne National Laboratory delivered a 1.6 GeV, pulsed ^{238}U beam on a 40 mg/cm^2 ^{180}Hf target, backed with 50 mg/cm^2 of natural Pb. The pulsed beam (82.5 ns) at an energy 15% above the Coulomb barrier, was chopped on two time ranges with on/off conditions of 8.25/16.5 μs and 2/4 ms, respectively. The recoils were stopped at the target position at the focus of the Gammasphere array, comprised of 98 γ-ray and three x-ray Compton-suppressed Ge detectors. The master trigger required at least one Ge detector to fire in the beam-off period. The delayed events were analyzed using γ-γ, γ- x-ray and γ-time coincidence matrices as well as a γ-γ-γ cube.

Several new transitions, in coincidence with lutetium x-rays, were observed with energies of 128, 141, 165 and 190 keV (see Fig. I-42). Gamma-ray coincidences were used to order these decays into a rotational sequence and crossover transitions were established for all but the 128 keV decay (see the inset of Fig. I-42). This band does not correspond to any previously known structure in lutetium nuclei.

Although there are insufficient statistics to obtain a decay curve for the new lutetium isomer, a limit of >1 ms was estimated for its half-life by comparing the relative intensity of the isomer on both the 16.5 μs and 4 ms time ranges. The transitions assigned to the lutetium band were found to be enhanced in the long-time range by a factor of ~2 compared with known millisecond isomers.

The observation of this millisecond high-K isomer in ^{180}Lu opens up the possibility of using `isomer tagging' to establish states above the isomer, enabling prompt γ-rays to be assigned from future deep-inelastic measurements and hence establish high-spin structures in the neutron-rich domain. Prompt spectroscopy could also extend the observed rotational band.

The results from this study were recently published.[2]

*University of Massachusetts-Lowell, †University of Surrey, United Kingdom, ‡University of Manchester, United Kingdom

[1] P. M. Walker and G. D. Dracoulis, Nature **399**, 35 (1999).
[2] C. Weldon *et al*., J. Phys. G **27**, L13 (2001).

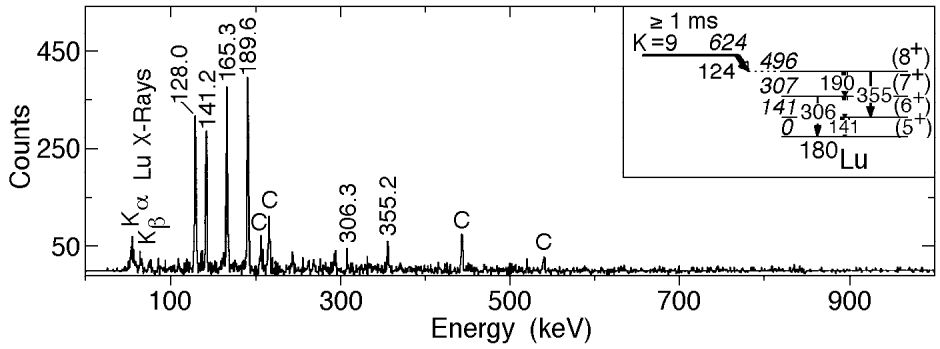

Fig. I-42. Gamma-ray coincidence spectrum produced from summing the coincidence spectra created by double-gating on transitions in the new band. The proposed level scheme is shown in the inset.

d.13. High-Seniority Intrinsic and Collective Structures in ^{174}Hf and ^{175}Hf

(F. G. Kondev, K. Abu Saleem, I. Ahmad, M. P. Carpenter, A. Heinz, R. V. F. Janssens, T. L. Khoo, T. Lauritsen, C. J. Lister, D. Seweryniak, I. Wiedenhöver, D. L. Balabanski,* P. Chowdhury,† D. M. Cullen,‡ M. Danchev,* G. D. Dracoulis,§ H. El-Masri,¶ T. M. Goon,* D. J. Hartley,* R. A. Kaye,|| L. L. Riedinger,* M. A. Riley,** I. Shestakova,† G. Sletten,†† P. M. Walker,¶ C. Wheldon,‡ and O. Zeidan*)

A characteristic feature of the rare-earth nuclei in the region near mass 180 is the dominance of high-Ω orbitals in the vicinity of both the neutron and proton Fermi surfaces. This gives rise to the presence of a number of high-K isomers which compete with structures formed by collective rotation along the yrast line. Recent investigations[1] show that the properties of rotational bands built on high-K states can be used as a tool to elucidate the influence of blocking of specific orbitals on pairing correlations.

A new study of ^{174}Hf and ^{175}Hf with Gammasphere at ATLAS aimed at identifying both high-seniority intrinsic and collective structures was carried out. The ^{130}Te(^{48}Ca,xn) reaction at a beam energy of 194 MeV was used. Several beam pulsing conditions were utilized which allowed highly sensitive measurements of γ rays across long-lived states to be performed. In ^{175}Hf (3n channel), the previously known bands[2] were confirmed and extended considerably in spin. Several new multi-quasiparticle structures were observed for the first time. The most notable being the bands built on the *seven*-quasiparticle $45/2^+$ (τ =2.8(1)μs), $47/2^+$ (τ < 3 ns) and $49/2^+$ (τ < 3 ns) states, and, more importantly, upon the $57/2^-$, and the $61/2^+$ (τ < 3 ns) *nine*-quasiparticle levels. The last two are the highest seniority intrinsic states with associated collective structures identified so far. A gamma-ray coincidence spectrum showing transitions above the $45/2^+$ isomer is presented in Fig. I-43. A mean-lifetime of τ = 32(3) ns was measured for the $57/2^-$ state, for which a limit of >10 ns was given before[2]. This isomer was known to have only ``anomalous" branches through members of the $35/2^-$ band[2]. In the current work, additional decays which obey the so-called K-selection rule (via the K^π = $47/2^+$ and $49/2^+$ high-K band members) were discovered. A detailed level scheme of ^{174}Hf (4n channel) was also constructed. The previously known structures were extended considerably in spin and new high-seniority bands were observed. No new long-lived states were discovered above the 14^+ *four*-quasiparticle isomer at 3312 keV.

In addition, comprehensive information on structures in neighboring ^{173}Hf and ^{176}Hf nuclei was also obtained. Analysis of the results continues at Argonne (^{175}Hf), Knoxville (^{174}Hf), Lowell (^{176}Hf) and Manchester (^{173}Hf).

*University of Tennessee-Knoxville, †University of Massachusetts-Lowell, ‡University of Manchester, United Kingdom, §Australian National University, Canberra, Australia, ¶University of Surrey, United Kingdom, ||Purdue University Calumet, **Florida State University, ††The Niels Bohr Institute, Roskilde, Denmark

1G. D. Dracoulis, F. G. Kondev and P. M. Walker, Phys. Lett. **B419**, 7 (1998).
2N. L. Gjørup *et al.*, Z. Phys. **A337**, 353 (1990).

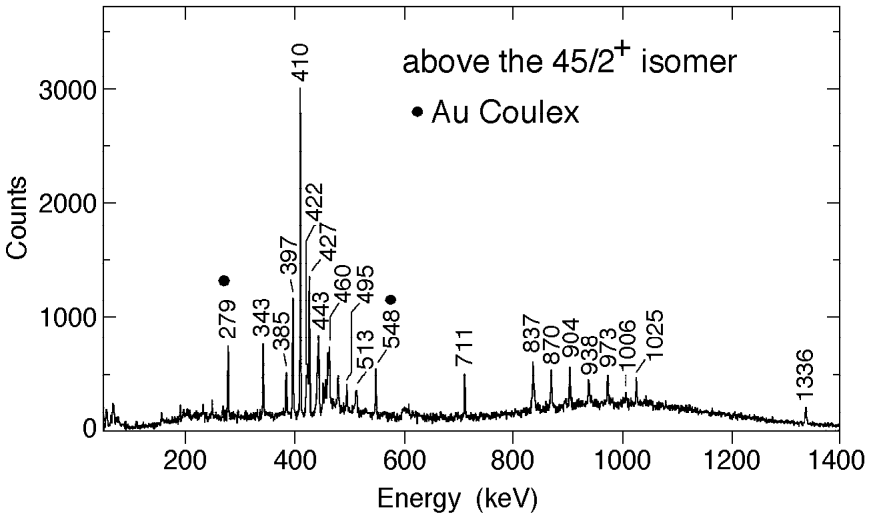

Fig. I-43. Spectrum of γ rays preceding delayed transitions below the 45/2+ isomer in ^{175}Hf.

d.14. Inelastic Excitation of New High-Spin Yrast Isomer in ^{180}Ta

(F. G. Kondev, I. Ahmad, M. P. Carpenter, R. V. F. Janssens, T. L. Khoo, C. J. Lister, D. Seweryniak, I. Wiedenhöver, P. Chowdhury,* I. Shestakova,* R. D'Alarcao,* C. Wheldon,† P. M. Walker,† C. J. Pearson,† Zs. Podolyak,† and D. M. Cullen‡)

Previous experiments to study the yrast structure of ^{180}Ta used light heavy-ion projectiles, namely, ^{11}B and ^{7}Li on targets of ^{176}Yb.[1] Several new isomers were observed using these partial fusion and fusion-evaporation reactions, including a 31 μs Kπ = 15- four-quasiparticle state.[2] However, this technique is limited to ~20 h of angular momentum. Recently, experiments using deep-inelastic reactions enabled states with spins up to ~30 h to be reached and K isomers were populated in neutron-rich nuclei that cannot be accessed using fusion-evaporation reactions with stable beams and targets.

For the first time, six-quasiparticle isomers were observed in the ^{180}Ta isotope at spins ~20 h. A partial level scheme for this nucleus is shown in Fig. I-44. Two new high-spin isomers were populated following deep-inelastic reactions with a pulsed ^{238}U beam incident on a thick ^{180}Hf target. Out-of-beam γ-ray events were collected using the Gammasphere germanium detector array. In addition to the known four-quasiparticle isomers, yrast Kπ = (22-) and K > 23 six-quasiparticle isomers were observed with microsecond half-lives. These are the highest-spin isomers observed using the technique of deep-inelastic excitation. The configurations assigned to the isomers are compared to predictions made by BCS and Lipkin-Nogami multiquasiparticle calculations. A full report of this work was published.[3]

*University of Massachusetts-Lowell, †University of Surrey, United Kingdom, ‡University of Manchester, United Kingdom

1G. D. Dracoulis, S. M. Mullins, A. P. Byrne, F. G. Kondev, T. Kibedi, S. Bayer, G. J. Lane, T. R. McGoram, and P. M. Davidson, Phys. Rev. C **58**, 1444 (1998).
2G. D. Dracoulis, F. G. Kondev, A. P. Byrne, T. Kibedi, S. Bayer, P. M. Davidson, P. M. Walker, C. Purry, and C. J. Pearson, Phys. Rev. C **53**, 1205 (1996).
3C. Wheldon *et al.*, Phys. Rev. C 62, 057301 (2000).

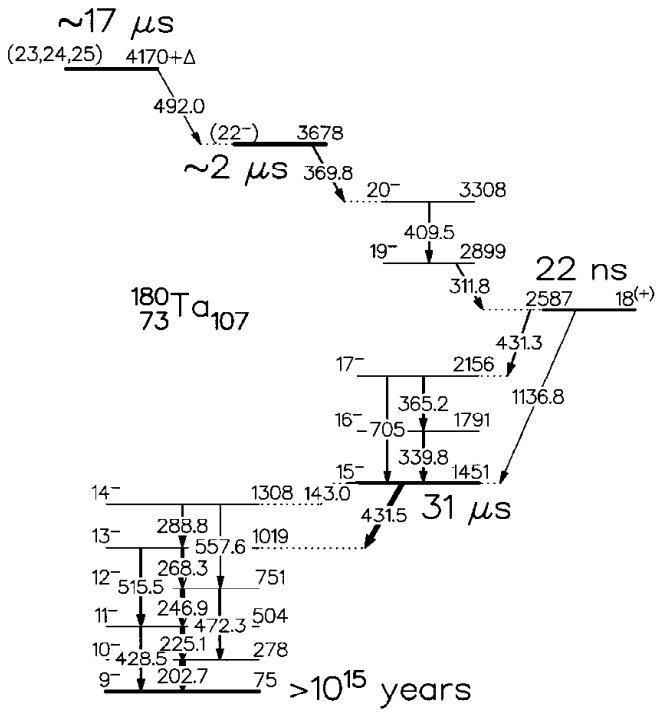

Fig. I-44. Partial level scheme of ^{180}Ta.

d.15. Interplay Between Octupole and Quasiparticle Excitations in ^{178}Hg and ^{180}Hg

(F. G. Kondev, K. Abu Saleem,* I. Ahmad, M. Alcorta, H. Amro,† L. T. Brown,§ M. P. Carpenter, J. Caggiano, C. N. Davids, A. Heinz, R. V. F. Janssens, R. A. Kaye,** T. L. Khoo, T. Lauritsen, C. J. Lister, J. Ressler,§§ D. Seweryniak,§§ S. Siem,††† A. A. Sonzogni,‡‡‡ J. Uusitalo,§§§ I. Wiedenhöver, P. Bhattacharyya,‡ S. M. Fischer,¶ B. Herskind,|| W. C. Ma,†† R. Nouicer,‡‡ W. Reviol,¶¶ L. L. Riedinger, |||| D. G. Sarantites,*** and P. G. Varmette††)

Analysis of the data on the even-even ^{178}Hg and ^{180}Hg nuclei was completed. Comprehensive level schemes were constructed for these isotopes, and that for ^{180}Hg is shown in Fig. I-45. Particular attention was paid to the low-lying negative parity excitations which are characterized by several distinctive features:

(a) the measured alignment at low frequency is ~3 h;
(b) the bands undergo a subsequent alignment gain of roughly 5 h at the noticeably low frequency of ~0.21 MeV;
(c) the $\Im(2)$ moments of inertia are larger than the corresponding values in the yrast band.

A careful inspection of the level schemes of the heavier even-even Hg isotopes with neutron number N = 98-106 reveals that in each nucleus a band of negative parity can be found with characteristics resembling closely those in ^{178,180}Hg. This observation can also be extended to the even-even Os and Pt isotones. Figure I-46 presents the excitation energies of the 5- through 13- members of the side-bands of interest in the three isotopic chains. Clearly, the variations with N of the excitation energies are small and very similar in all the nuclei under consideration. This behavior argues against a pure two-quasiparticle character for these structures, and supports their association with octupole vibrations. The enhancement of the latter at low spin in this mass region comes as no surprise because of the presence of pairs of orbitals with $\Delta j = \Delta l = 3$ h near both the proton and the neutron Fermi surfaces. The microscopic structure of the octupole phonon is rather complex and the specific configurations were recently discussed in detail in Ref. 1. It was suggested[1], for example, that the proton $i_{13/2} \otimes f_{7/2}$ coupling will be an important component. If so, the shape driving effects of the $\pi i_{13/2}$ orbital will remain strong and the nuclear shape associated with the low-spin part of the

negative parity bands may well be similar to the one associated with the two-quasiproton configuration. Thus, the deformation would be somewhat different from that of the vacuum configuration. This, in turn, would provide a qualitative explanation for the fragmented decay of the negative parity bands observed at low spin.

A full report of this work was published[2].

*Argonne National Laboratory and Illinois Institute of Technology, †Argonne National Laboratory and Mississippi State University, ‡Purdue University, §Argonne National Laboratory and Vanderbilt University, ¶DePaul University, ||The Niels Bohr Institute, Denmark, **Argonne National Laboratory and Purdue University Calumet, ††Mississippi State University, ‡‡University of Illinois at Chicago, §§Argonne National Laboratory and University of Maryland, ¶¶University of Tennessee-Knoxville and Washington University-St. Louis, ||||University of Tennessee-Knoxville, ***Washington University-St. Louis, †††Argonne National Laboratory and University of Oslo, Norway, ‡‡‡Argonne National Laboratory and National Nuclear Data Center, §§§Argonne National Laboratory and University of Jyväskylä, Finland

1F. G. Kondev *et al*., Phys. Rev. C **61**, 044323 (2000).
2F. G. Kondev *et al*., Phys. Rev. C **62**, 044305 (2000).

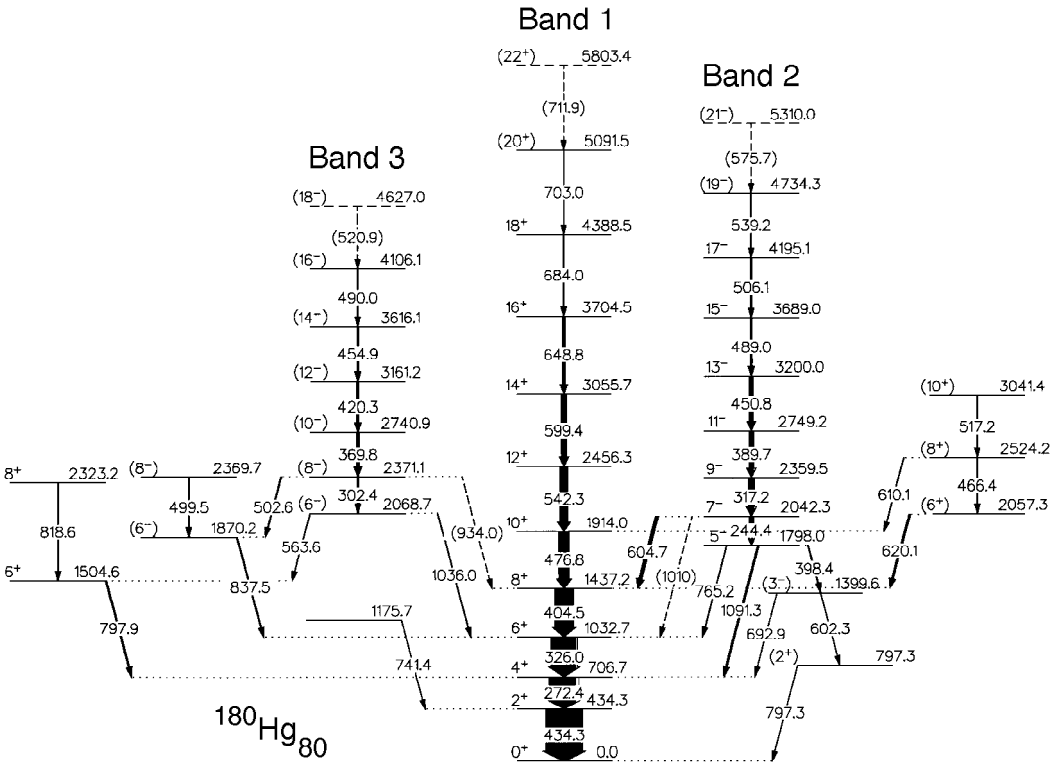

Fig. I-45. Proposed ^{180}Hg level scheme. Quantum numbers are given under parenthesis when reliable multipolarity information was not obtained. For each transition, the width of the arrow is proportional to the measured intensity.

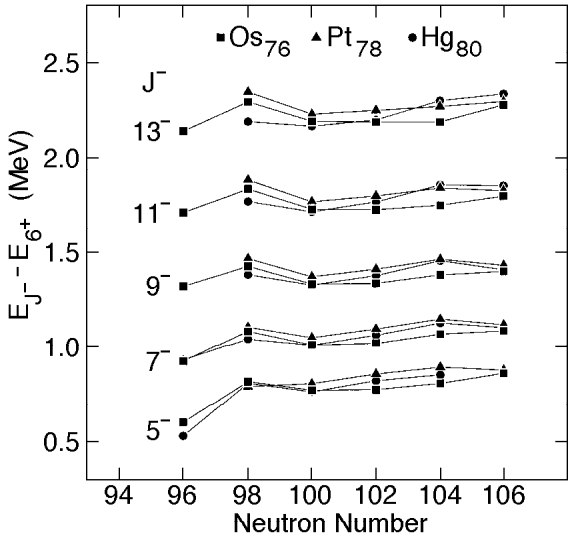

Fig. I-46. Excitation energies for the 5⁻, 7⁻, 9⁻, 11⁻ and 13⁻ levels relative to the 6⁺ member of the ground state band for the structures in Os, Pt and Hg even-even nuclei.

d.16. Shape Competition and Octupole Correlations in Light Even-Even Pt Nuclei

(F. G. Kondev, K. H. Abu Saleem, I. Ahmad, M. P. Carpenter, A. Heinz, R. V. F. Janssens, T. L. Khoo, T. Lauritsen, C. J. Lister, G. L. Poli, J. Ressler, D. Seweryniak, I. Wiedenhöver, M. Danchev,* T. M. Goon,* D. J. Hartley,* L. L. Riedinger,* W. C. Ma,† H. Amro,† W. Reviol,‡ J. A. Cizewski,§ and M. B. Smith§)

The proximity of the $Z = 82$ and $N = 82$ spherical shell gaps, along with the presence of the deformation driving $\pi i_{13/2}$ and $\pi h_{9/2}$ orbitals, create a battlefield for shape competition in light ($A \approx 174$) $_{78}$Pt nuclei. Indeed, the unusual low-spin interactions observed in the ground-state bands of ^{176,178}Pt[1] were described as a result of a 'more-deformed' vacuum configuration crossing the initial, less-deformed ground-state sequence. In addition, negative-parity sidebands were observed in several light Os, Pt, and Hg even-even nuclei, where octupole correlations were invoked for their configurations at lower spins.[2] In order to investigate these phenomena further, an experiment was performed to populate high-spin states of ^{172,174,176}Pt.

The experiment was performed at ANL with the ATLAS facility providing the ^{84}Sr beam. Several reactions were used to produce these very neutron-deficient nuclei, which included ^{92}Mo(^{84}Sr,2p2n)^{172}Pt, ^{92}Mo(^{84}Sr,2p)^{174}Pt, ^{94}Mo(^{84}Sr,2p2n)^{174}Pt, ^{94}Mo(^{84}Sr,2p)^{176}Pt, and ^{96}Mo(^{84}Sr,2p2n)^{176}Pt. Prompt γ-rays were detected with the Gammasphere array, consisting of 101 Ge detectors. A multi-wired proportional avalanche counter (PPAC) located at the focal plane of the FMA provided the *A/Q* information and the time of arrival of residues. The recoils were implanted in a double-sided silicon detector (DSSD), where subsequent alpha decays were measured. Correlating these alpha decays with the implanted residues enable us to associate γ-rays with the proper recoils. This method is commonly referred to as recoil decay tagging (RDT).[3]

The use of Gammasphere allowed for a relatively high-statistic data set to be taken on ^{172}Pt as compared with the previous two studies.[4,5] An $E_\gamma \times E_\gamma$ matrix was created where the gamma rays were correlated with the alpha decay associated with ^{172}Pt. Coincidence relationships and measured intensities of the γ rays resolved the discrepancy between the two previous reports on the ordering of some of the transitions favoring that of Ref. 4. A new collective structure was also established, which feeds the 4^+ level in the ground-state sequence.

A matrix sorted with gamma rays that were correlated with A = 174 recoils allowed for the ground-state band to be significantly extended from $I = 14^+$ (Ref. 6) to 24^+ in ^{174}Pt. In addition, three new sidebands were observed and assigned negative parity based on systematics in the Pt nuclei. An A = 176 mass-gated matrix enabled the extension of the two known sidebands[1] as well as establishment of a new third sideband.

In all three of these nuclei, low-spin crossings are observed in the ground-state bands and are associated with the crossing of the more-deformed vacuum configuration. However, the crossing frequency is found to increase from $\hbar\omega_C \approx 0.15$ MeV for ^{176}Pt, 0.24 MeV for ^{174}Pt, and >0.29 MeV for ^{172}Pt. This is likely the result of the deformed prolate minimum increasing in excitation energy as the nuclei near the N = 82 spherical shell gap. It is also possible that the prolate minimum has smaller deformation as the neutron Fermi is decreased. This latter possibility will be investigated with the use of a two-band mixing calculation.

*University of Tennessee-Knoxville, †Mississippi State University, ‡Washington University-St. Louis, §Rutgers University

1G. D. Dracoulis *et al*., J. Phys. G **12**, L97 (1986).
2F. G. Kondev *et al*., Phys. Rev. C **61**, 044323 (2000).
3E. S. Paul *et al*., Phys. Rev. C **51**, 78 (1995).
4B. Cederwall *et al*., Phys. Lett. **B443**, 69 (1998).
5D. Seweryniak *et al*., Phys. Rev. C **58**, 2710 (1998).
6G. D. Dracoulis *et al*., Phys. Rev. C **44**, R1246 (1991).

d.17. Spectroscopy of Neutron-Deficient Odd-Mass ^{173,175}Pt Nuclei

(F. G. Kondev, K. Abu Saleem,* I. Ahmad, M. Alcorta, H. Amro,† M. P. Carpenter, C. N. Davids, A. Heinz, R. V. F. Janssens, T. L. Khoo, T. Lauritsen, C. J. Lister, G. L. Poli, J. Ressler,|| D. Seweryniak,|| I. Wiedenhöver, J. A. Cizewski,‡ M. Danchev,§ D. J. Hartley,§ W. C. Ma,¶ W. Reviol,** L. L. Riedinger,§ and M. B. Smith‡)

Analysis of the level schemes for ^{173}Pt and ^{175}Pt covered in last year's Annual Report was completed. The results were obtained from an extensive set of measurements using fusion reactions of ^{84}Sr ions with ^{92}Mo and ^{94}Mo targets. Prompt γ rays were detected with the Gammasphere array in conjunction with the recoil-decay tagging technique, after mass selection.

The new data clearly establish competing triaxial and prolate structures in the ^{175}Pt (N = 97) isotope. Their properties match closely those of ^{179}Hg (see the contribution to this year's Annual Report), with the exception that the oblate minimum rises significantly in energy at Z = 78 and has not been observed. Excited bands in ^{175}Pt, most likely of negative parity, feeding directly the 7/2- ground state were observed for the first time. In addition, we extended the previously known $\nu i_{13/2}$ yrast band[1] in spin and we placed the $13/2^+$ bandhead at 171 keV above the ground state. With two neutrons less, however, the yrast structure of ^{173}Pt (N = 95) is dominated by a single ΔI = 2 band which is assigned a low-Ω $i_{13/2}$ neutron configuration. Its deformation is lower than that found for the corresponding band in ^{175}Pt, as evident from the systematics of transition energies shown in Fig. I-47. The decline in deformation below mid-shell occurs in a rather smooth way as the neutron number decreases. This can be partially attributed to the stepwise emptying of the low-Ω $i_{13/2}$ *neutron* intruder orbitals.

*Argonne National Laboratory and Illinois Institute of Technology, †Argonne National Laboratory and Mississippi State University, ‡Rutgers University, §University of Tennessee-Knoxville, ¶Mississippi State University, ||Argonne National Laboratory and University of Maryland, **University of Tennessee-Knoxville and Washington University-St. Louis

1B. Cederwall *et al*., Z. Phys. **A337**, 283 (1990).

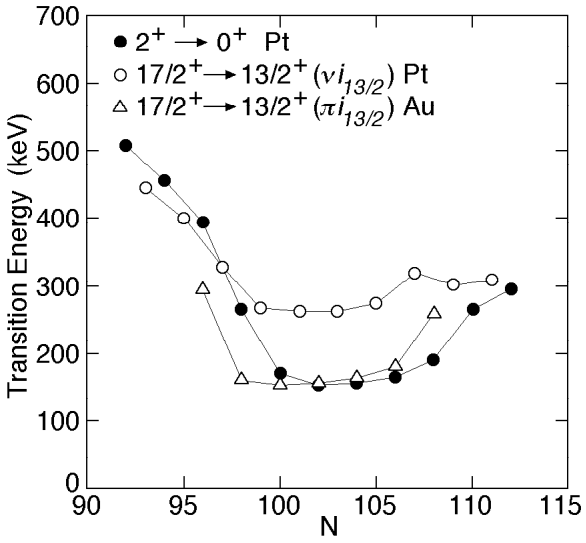

Fig. I-47. Systematics of transition energies for selected Pt and Au isotopes.

d.18. Excited Rotational Bands in the Superdeformed Well of ^{194}Hg

(T. L. Khoo, I. Ahmad, M. P. Carpenter, F. Hannachi, R. V. F. Janssens, A. Lopez-Martens*, T. Lauritsen, A. Korichi,* T. Dossing,† and B. Herskind†)

Numerous discrete superdeformed (SD) bands were identified, so that the properties of cold SD states were well studied. In contrast, there is little information on the properties of excited states in the SD minimum. In the Hg nuclei, we identified that there is strong collective quasicontinuum E2 peak, which feeds the yrast SD bands. It is interesting to establish the collectivity, moments of inertia and rotational spreading widths of excited states within the SD well. One might naively expect that the rotational spreading widths of excited SD bands might be larger than those of normal-deformed states because there are two sources, which contribute to spread the collective strength. In addition to the interaction among the dense excited SD states by the residual 2-body interaction, excited SD states can also couple readily to the hot normal-deformed states on the other side of the barrier separating the two classes of states.

We constructed gamma-gamma matrices after setting pairwise gates on transitions of the yrast SD band in ^{194}Hg. In addition to the square grid of dots corresponding to the SD lines, three continuous ridges parallel to the diagonal are seen for the first time in the feeding of a SD band. The widths of the ridges are very narrow, <10 keV, immediately indicating very small spreading widths of the rotational strength. Although the transitions along the ridge emanate from excited states, which have complex wavefunctions with many components, nonetheless states with spins different by 2h are very similar. These excited SD rotational bands may represent examples of the ergodic bands proposed by Mottelson.

*CSNSM, IN2P3-CNRS. Orsay, France
†Niels Bohr Institute, Copenhagen, Denmark

d.19. BaF_2 Collaboration to Measure High Energy γ Rays

(T. L. Khoo, B. B. Back, M. P. Carpenter, P. Collon, A. M. Heinz, D. J. Henderson, D. G. Jenkins, M. P. Kelly, F. G. Kondev, C. J. Lister, T. O. Pennington, R. H. Siemssen, D. Seweryniak, V. Nanal,* D. J. Hofman,† I. Dioszegi,‡ A. Bracco,§ F. Camera,§ M. Halbert,¶ R. Varner,¶ K. Eisenman,|| P. Heckman,|| J. Seitz,|| M. Thoennessen,|| U. Garg,** B. McClintock,†† R. J. van Swol,†† and S. Mitsuoka‡‡)

We have initiated a program to study the properties of hot nuclei with well-defined specification of mass, spin and excitation energy. This unique study was performed in a collaboration with participants from Argonne, Oak Ridge, Michigan State University, Texas A&M University, Tata Institute for Fundamental Research, Stony Brook, Notre Dame University, and INFN Milano. The BaF_2 detectors were supplied by Oak Ridge, Michigan State and Texas A&M. A total of 148 BaF_2 crystals were mounted in four packs of 37 detectors centered at angles of ±90 and ±121 degrees with respect to the beam axis and mounted at the target position in front of the Fragment Mass Analyzer, see Fig. I-48.

The advantage of this arrangement is that it is possible to uniquely identify the mass of the γ-emitting nuclei as they are detected in the focal plane of the FMA. In addition, the Argonne-Notre Dame BGO array, consisting of 50 crystals, was mounted at the target position, see Fig. I-49, to provide information on the total γ-ray energy and multiplicity of the final γ-ray cascade to further define the entry distribution in angular momentum and excitation energy of the fusion product. For a given decay channel at different bombarding energies, it is thus possible to map out a wide range of angular momentum region while keeping the excitation energy above the yrast line similar.

A new target chamber was designed and built. It contains an APEX style target-wheel, which can be rotated up 600 RPM to avoid melting of the target material with intense heavy-ion beams. This chamber also housed a Faraday cup/aperture assembly used for tuning the beam onto the target position as well as mounts for two Si monitor detectors and a reset foil. A photograph of the target region is shown in Fig. I-49.

Aside from a commissioning experiment needed to shake down electronics and the data-acquisition system, five experiments were carried out during 2000. The physics topics were chosen to study the emission of high-energy γ-rays in different areas of the nuclear chart and of different ground state shapes. In one study, we chose three nuclei, namely Sn, Er and Dy to represent different mass regions likely to be sensitive to different mechanisms responsible for the broadening of GDR width. We selected spherical nuclei, stiff deformed nuclei and transitional nuclei, with the goal of studying different physics in one consistent experimental setup, and with one consistent method of analysis. This approach should serve to reduce experimental systematic differences.

These efforts constitute the most comprehensive systematic investigation of the GDR spectra from hot nuclei in exclusive measurements. Subsequently, nuclei ranging in mass from ^{118}Sn to ^{224}Th were studied. The five experiments are described below in more detail.

*Argonne National Laboratory and University of Illinois at Chicago, †University of Illinois at Chicago, ‡SUNY at Stony Brook, §University of Milan, Italy, ¶Oak Ridge National Laboratory, ||Michigan State University, **University of Notre Dame, ††ANL Summer Student, ‡‡JAERI Advanced Science Research Center, Tokyo, Japan

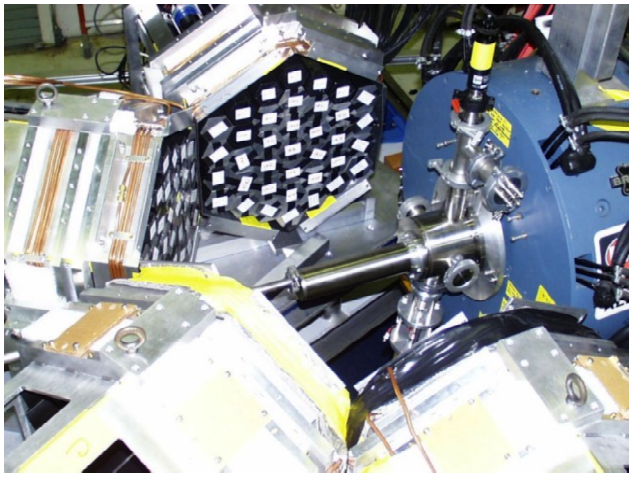

Fig. I-48. Photograph of the target region showing the four BaF_2 detector packs , the target chamber and the first quadrupole magnet of the FMA. Beam enters from the left.

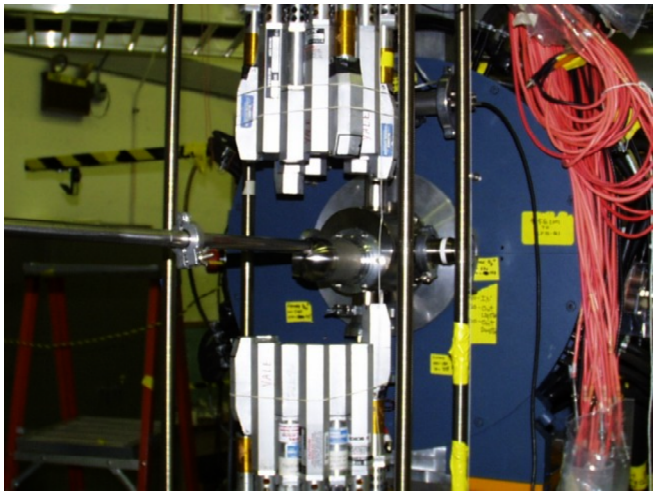

Fig. I-49. Photograph of the BGO array at the target position. The vertical position of the individual BGO crystals were for the running configuration adjusted to provide maximal solid angle without shadowing the BaF_2 detectors.

d.20. The GDR Structure in Sn Nuclei from Highly Exclusive Studies

(T. L. Khoo, B. B. Back, M. P. Carpenter, P. Collon, D. J. Hofman, D. Jenkins, M. P. Kelly, F. G. Kondev, T. Lauritsen, V. Nanal, T. Pennington, and R. H. Siemssen)

Measurements of GDR γ-rays and evaporation residues produced in ^{40}Ar + ^{74}Ge reactions at bombarding energies of 125 and 150 MeV leading to the compound nucleus ^{114}Sn were completed. The aim was to investigate the evolution of the GDR, particularly the width, at moderate but well defined values of excitation energy and spin. In a spherical nucleus at zero temperature the GDR is not split into two components by deformation. Therefore, it is more straightforward to investigate the temperature-induced shape fluctuations of away from sphericity. The study is based on γ-rays detected in coincidence with specific evaporation residues formed largely in ^{74}Ge(^{40}Ar,xn) reactions. Results of this technique will be compared to those using the γ-ray multiplicity technique of Ref. 1.

Approximately 140 hours of coincidence data were collected in two separate experimental runs using the LEPPEX BaF_2 array, FMA, and BGO sum-energy array. Several thousand high-energy GDR γ-ray coincidence events were collected at each bombarding energy.

A principal experimental concern was the energy gain stability of the 148-element LEPPEX array. Analysis of systematic energy calibrations collected periodically using ^{88}Y γ-rays indicates typical energy gain shifts of less than 5% for nearly all detectors over the 3-4 day periods. These shifts may be properly corrected for using the known ^{88}Y peak positions.

Preliminary spectra for evaporation residues and γ-rays detected in coincidence with A = 110 residues are shown in Figures I-50 and I-51 for 150-MeV bombarding energy. Statistical model calculations using the CASCADE code indicate that these γ-rays associated with mass A = 110 are emitted primarily from compound nuclei formed in a spin region centered around I ~45 h with a width of I ~15 h. A detailed analysis of γ-ray data for A = 110 at 150 MeV bombarding energy and A = 111 at 125 MeV, which represent the two widely separated values of initial compound nucleus angular momentum will be performed. Both data sets were measured here with good statistical accuracy.

[1]M. Mattiuzzi *et al*., Nucl. Phys. **A612**, 262-278 (1997).

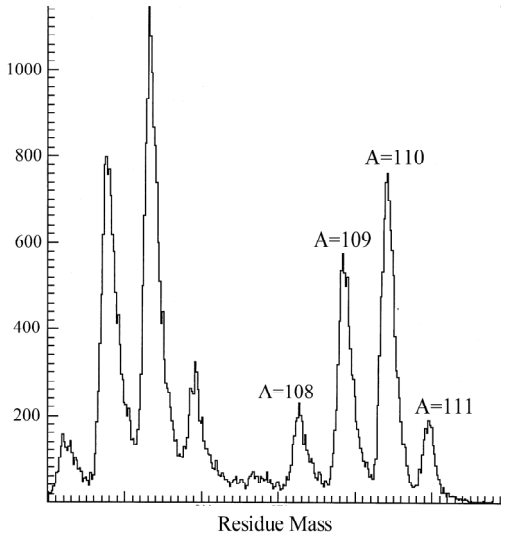

Fig. I-50. Measured evaporation residue mass spectrum (left) for ^{40}Ar + ^{74}Ge at 150 MeV bombarding energy.

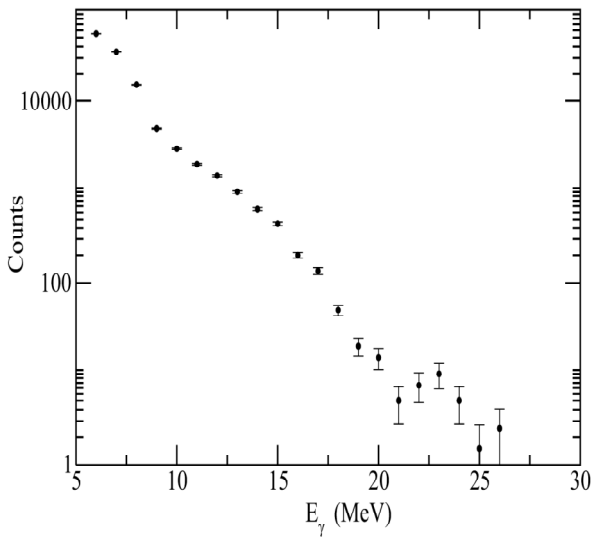

Fig.I-51. Measured γ-ray spectrum from Sn and neighboring elements with A = 110 using the LEPPEX array.

d.21. GDR Studies in Exclusively Tagged Er Isotopes (T. L. Khoo, B. B. Back, M. P. Carpenter, P. Collon, D. J. Hofman, D. Jenkins, M. P. Kelly, F. G. Kondev, T. Lauritsen, V. Nanal, T. Pennington, and R. H. Siemssen)

We have measured the high energy γ-rays from ^{164}Er in coincidence with the evaporation channels (4n,5n,6n). The ^{164}Er is a well-deformed nucleus. With increasing temperature, shape fluctuations will appear but the spread will be less than that for transitional nucleus. There are theoretical predictions indicating a rapid increase in the width of the GDR at high spin. The experiment was carried out using ^{40}Ar beams from ATLAS of energy 163 and 187 MeV on a ^{124}Sn target. A combination of a target wheel rotation and beam wobbling was used to prevent target deterioration due to high beam currents (10 pnA). The excellent beam timing (< 700 ps) allowed a clean n-γ separation. Different decay channels 4n-6n are clearly separated in the FMA focal plane. The sum energy and multiplicity of the γ-ray cascade are also measured in the BGO array. Figure I-52 shows the γ-ray spectra from the 4n and 6n decay channels at E_{beam} = 187 MeV. A preliminary analysis also indicates that there are differences in the γ-ray spectra gated with 4n channel at the two bombarding energies. The experimental spectra will be compared with theoretical spectra, which originate from the same region of spin and excitation energy. This same approach will be used in analysis of the data from hot Sn and Dy nuclides.

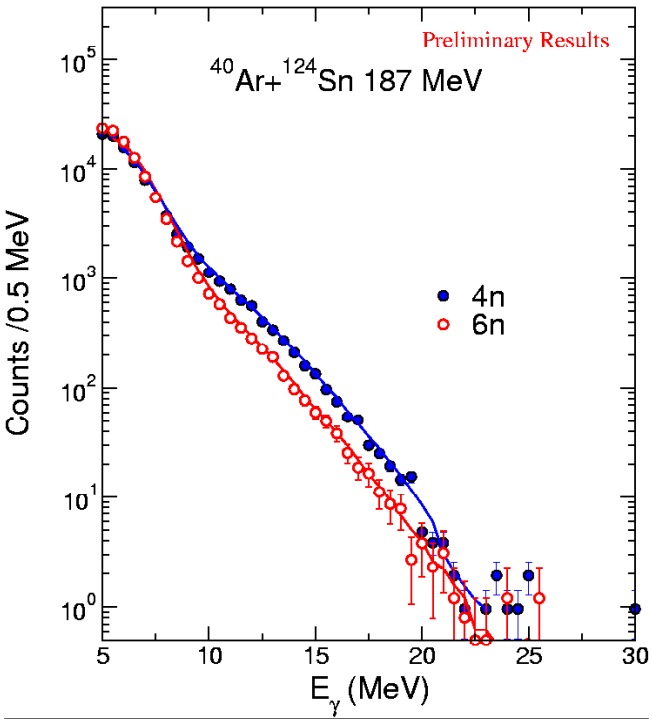

Fig. I-52. γ-ray spectra gated on the 4n (solid points) and 6 n (open circles) observed in the 187 MeV $^{40}Ar + ^{124}Sn$ reaction. Note the difference in shape between the two evaporation channels.

d.22. Structure of Hot Dy Nuclei as a Function of Spin and Excitation Energy (T. L. Khoo B. B. Back, M. P. Carpenter, P. Collon, D. J. Hofman, D. Jenkins, M. P. Kelly, F. G. Kondev, T. Lauritsen, V. Nanal, T. Pennington, and R. H. Siemssen)

The properties of hot transitional nuclei are particularly interesting since they undergo a shape transition from prolate to oblate shapes at relatively low excitation energies. The near-yrast states in these nuclei exhibit both collective and single particle properties, which are associated with deformed and oblate shapes, respectively. Mean field-theory predicts a phase transition from prolate rotation to oblate, aligned particle motion with increasing spin.

The experiment was carried out using ^{32}S beam of E = 140 MeV, 167 MeV on a rotating ^{124}Sn target. The high-energy gamma-ray spectra in coincidence with 4n, 5n decay channel was recorded. The γ-ray spectra for the 4n channel at the two bombarding energies were obtained. Detailed theoretical analysis using spin-energy dependent strength functions will be carried out.

d.23. Hot GDR in ^{118}Sn (T. L. Khoo, B. B. Back, M. P. Carpenter, D. J. Hofman, M. P. Kelly, V. Nanal, T. Pennington, R. H. Siemssen, P. Heckman,*and M. Thoennessen*)

Experiments were run in the past to measure properties of the giant dipole resonance (GDR) in Sn isotopes.[1,2] In these experiments the GDR was studied from the γ-decays of the full decay cascade. Consequently, the γ-ray spectra contain information on the daughter nuclei populated at different temperatures in addition to the nucleus of interest itself. Thus, to extract the parameters of the GDR it was necessary to average over many decay steps. This procedure introduces uncertainties, because it requires knowledge of

uncertain key parameters. It is because of these uncertainties that a measurement of the GDR should be made in such a way as to eliminate averaging over many decay steps.

In December of 2000, an experiment was performed to measure the GDR in ^{118}Sn. This experiment was designed to eliminate averaging over many decay steps, and thus allow for the first direct comparison of the hot GDR with the ground state measurement in the same nucleus. Consequently, the width and energy of the GDR will be determined more accurately than in the past. This measurement required measuring the γ-ray spectrum for the nucleus following one-neutron evaporation (i.e. ^{117}Sn) at the corresponding excitation energy. Subtracting the ^{117}Sn γ-ray spectrum from ^{118}Sn will yield the γ-ray spectrum from the initial compound nucleus only. This technique was previously used successfully to study ^{162}Yb (Ref. 3).

The ^{118}Sn and ^{117}Sn compound nuclei were formed using the fusion evaporation reactions ^{18}O + ^{100}Mo and ^{17}O + ^{100}Mo. We excited the ^{118}Sn nucleus to 85 MeV and the ^{117}Sn nucleus to 71 MeV. This required beam energies of 95 MeV and 79 MeV respectively. The ^{100}Mo target was approximately 0.5 mg/cm2 thick. Beam currents of approximately 15 pnA were used. The experiment ran for a total of five days.

The GDR of the compound nucleus will be extracted by studying the data collected from the expanded LEPPEX array of BaF_2 detectors from ORNL, MSU, and TAMU. These data will yield the GDR decay via γ rays. Coincidences with the FMA ensured the formation of the compound nucleus. In order for the difference technique to be well-defined, it is necessary to keep the range of angular momenta the same for the ^{118}Sn and ^{117}Sn γ-ray spectra. This will be accomplished by using the data collected from the BGO detectors and/or making mass cuts on the FMA data.

The analysis of the data from this experiment is currently underway.

*Michigan State University

1E. Ramakrishnan *et al*., Phys Rev. Lett. **76**, 2025 (1996).
2M. P. Kelly *et al*., Phys. Rev. Lett. **82**, 3404 (1999).
3A. Maj *et al*., Phys. Lett. **B291**, 385 (1992).

d.24. Hot GDR and Dissipation in ^{224}Th

(T. L. Khoo, B. B. Back, M. P. Carpenter, D. J. Hofman, M. P. Kelly, V. Nanal, T. Pennington, R. H. Siemssen, J. Seitz,* P. Heckman,* and M. Thoennessen*)

The experiment was designed to measure the spin distribution and GDR strength function of highly excited ^{224}Th in coincidence with evaporation residues. Standard statistical model calculations do not predict any evaporation cross section, but the fission probability at high excitation energy can be reduced due to dissipation. In ^{16}O + ^{208}Pb fusion reactions evaporation residue cross sections of ~10 mb were measured.[1] The temperature and/or deformation dependence of the dissipation is still an open question remaining to be solved.[2,3] The spin distribution leading to evaporation residues as well as the shape of the GDR are sensitive measures whether dissipation is dominated from inside or outside the fission barrier.

The experiment was carried out with a ^{48}Ca beam on a 810 μg/cm^2 ^{176}Yb target. The beam energies were 256 MeV, 219 MeV and 206 MeV with currents ranging between 30-70 nA.

The evaporation residue cross section for the ^{48}Ca induced reaction was about a factor 200 smaller than the previously measured ^{16}O reaction. Thus the GDR was only measured at 256 MeV. Data for the spin distribution were taken at all three energies.

The analysis of this experiment is in progress.

*Michigan State University

1K.-T. Brinkmann *et al.*, Phys. Rev. C **50**, 309-316 (1994).
2N. P. Shaw *et al*., Phys. Rev. C **61**, 044612 (2000); I. Dioszegi *et al*., Phys. Rev. C **46**, 627 (1992), and references therein.
3P. Fröbrich and I. I. Gontchar, Phys. Rep. **292**, 131 (1998).

d.25. High-Energy Photons from Very Symmetric Reactions: The Giant Dipole Resonance in Highly Rotating Cold Nuclei

(T. L. Khoo, B. B. Back, M. P. Carpenter, A. M. Heinz, D. J. Hoffman, R. V. F. Janssens, F. G. Kondev, T. Lauritsen, W. Lopez-Martens, V. Nanal, A. Bracco,* F. Camera,* I. Dioszegi,† F. Della Vedova,* S. Leoni,* B. Million,* M. Pignanelli,* M. Thoennessen,† R. Verner,‡ and O. Wieland*)

Symmetric fusion reactions of two nearly closed shell medium heavy nuclei have the peculiar feature of leading to very cold compound nuclei at high angular momentum and are expected to be very dissipative and slow. In addition, reactions of this type were shown to lead to radiative fusion, namely to the formation of a composite nucleus deexciting to its ground state without the evaporation of nucleons. There are two possible and different mechanisms leading to "radiative fusion". One consists of the direct capture process in which an entrance channel configuration involves the emission of a single gamma ray populating "directly" the compound nucleus. The second mechanism consists of a two step process, namely the formation of the compound nucleus by fusion reaction and the 0 nucleon channel is one of the possible decay mode together with particle evaporation with all the particle and gamma-decay modes obeying statistical laws.

The investigation of the nature of the "radiative fusion" process requires the measurement of the population yields of the different residual channels. The additional measurement of the energy spectra of the decay products is expected to provide a more stringent test on the statistical nature of the process. In particular, from the study of the high energy γ-ray spectra associated with the different residual nuclei one expects to obtain information on whether or not these very symmetric and cold reactions can be described with the same standard statistical model which was used successfully to described the more asymmetric and hotter reactions among heavy ions.

The measurement of high energy γ-ray emitted by the reaction ^{90}Zr + ^{89}Y at a bombarding energy of 352 MeV was made. Some preliminary results are shown in Figs. I-53 and I-54. It is interesting to note that the distribution of the residual nuclei is strongly changed when a high energy γ-ray is detected in coincidence (see Fig. I-53). Also the shapes of the high energy spectra associated to the different residual nucleus channels are different. These two facts reflect the different phase space sampled by the high energy γ-rays when cascades leading to different residual nuclei are selected. The analysis of the data is in progress.

*Università degli Studi di Milano and INFN, Italy †Michigan State University, ‡Oak Ridge National Laboratory

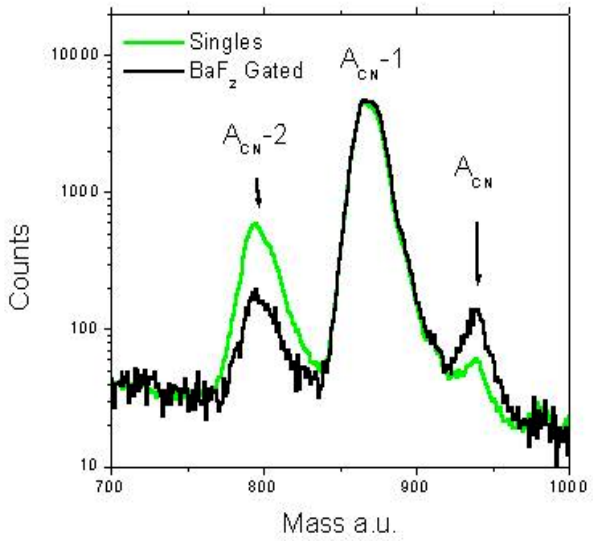

Fig. I-53. Mass spectra observed in the FMA focal plane without (green) and with (black) a coincidence gate on the BaF_2 array.

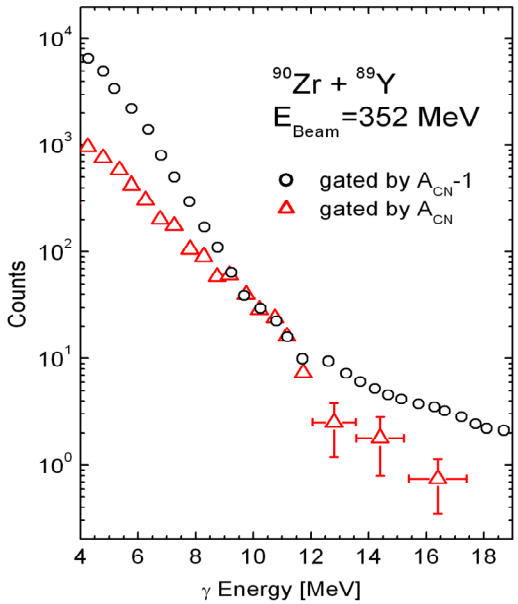

Fig. I-54. γ-ray spectra observed in the ^{90}Zr + ^{89}Y reaction at 352 MeV in coincidence with the 0n channel (open triangles) and 1n channel (open circles), respectively.

d.26. A New Phenomenon in Heavy-Ion Fusion Reactions at Very Low Cross Sections

(C. L. Jiang, H. Esbensen, and K. E. Rehm)

Sub-barrier fusion cross sections between heavy ions were studied extensively since the first observation that the fusion probability can be strongly enhanced compared to one-dimensional tunneling calculations.[1] The enhancement can be explained by channel-coupling effects which create a multi-dimensional potential barrier, resulting in an increased tunneling probability. In most experiments, fusion cross sections were measured down to the 0.1 - 1 mb region, and for numerous systems they are successfully described by coupled-channels calculations. We are interested in even lower fusion cross sections and want to investigate whether there are any new phenomena and what are the reaction mechanisms. A better understanding of the fusion process at these energies is also important in connection with other measurements where reactions with very small fusion probabilities are investigated, e.g. in the production of superheavy elements.[2]

In order to eliminate the strong energy dependence of the measured cross sections in low energy light ion reactions, people have introduced the so called S-factor, defined as $S(E) = \sigma \cdot E \exp(2\pi\eta)$, where η is the Sommerfeld parameter $\frac{Z_1 Z_2 e^2}{h\nu}$. At very low energies, S(E) is often nearly independent of the energy, as seen, for example, in ^{3}He(α,γ)^{7}Be (Ref. 3) and ^{12}C + ^{16}O (Ref. 4) reactions. At higher energies, $log(S(E))$ shows a linear increase towards lower energy which can be understood from the penetrability through an l = 0 barrier.[5]

For heavier systems, there are only few experiments that measured fusion cross section below the 0.1 - 1 mb region. An interesting behavior is observed when we convert the data into an S-factor. Some results are shown in Fig. I-55 as functions of the excitation energy in the compound nucleus. For ^{90}Zr + ^{96}Zr, the S-factor increases exponentially with decreasing energy, while for ^{90}Zr + ^{90,92}Zr,^{89}Y, a "bend-over" is observed, and in one case (^{90}Zr) there are even indications of some oscillations at the lowest energies. Up till now, there are only two other heavy systems which clearly show a bend-over in the S-factor, namely, ^{16}O + ^{144}Sm (Ref. 7) and ^{58}Ni + ^{58}Ni (Ref. 8).

There are eight other systems for which the S-factor seems to bend over at low energy.[7,12,13] They are collected in Table 1, and some of them are shown in Fig. I-55. Table 1 gives the energy E_0 and the associated cross section $\sigma(E_0)$, where the bend-over takes place in the 5+8 systems mentioned above. It is worthwhile to point out some interesting features related to the bend-over:

a) The phenomenon occurs at very low cross sections (typically ~ 1-100 μb),where coupled-channels effect are expected to be small.

b) The energy E_0 and cross section $\sigma(E_0)$ at which $log(S(E))$ bends over can be determined quite accurately.

c) The phenomenon is strongly system dependent.

All of the systems, for which the bend-over phenomenon was seen so far, involve at least one closed shell nucleus. It is of interest to know the energy E_0 at which the bend-over occurs in other systems, and what nuclear structure information determines it. Eventually for heavy systems, the cross section (and thus $S(E)$) will vanish when the available energy becomes less than the energy of the ground state compound nucleus, while for light systems the cross section (but not the $S(E)$) will vanish when the energy becomes zero.

It is of interest to study this new phenomenon, which so far lacks a detailed theoretical understanding. We plan to determine fusion excitation functions down to the 100 nb region using an efficient method that we recently developed.[15] The method consists of measuring the velocity-distribution of evaporation residues at zero-degree from which the total angle-integrated cross section can be determined.

1M. Beckerman, Rep. Prog. Phys. **51**, 1047 (1988); R. Vandenbosch, Ann. Rev. Nucl. Part. Sci. **42**, 447 (1992).
2S. Hofmann *et al*., Z. Phys. **A358**, 377 (1997).
3H. Krawinket *et al*., Zeit. Phys. **A304**, 307 (1982).
4B. Cujic *et al*., Nucl. Phys. **A266**, 461 (1976).
5M. Baranger and E. Vogt, Advances in Nuclear Physics, vol. 4 (Plenum Press. New York, 1968) p. 133-204.
6J. G. Keller *et al*., Nucl. Phys. **A452**, 173 (1987).
7R. G. Stokstad *et al*., Phys. Rev. C **21**, 2427 (1980).
8M. Beckerman *et al*., Phys. Rev. C **23**, 158 (1981) and Phys. Rev. C **25**, 837 (1982).
9W. Reisdorf *et al*., Nucl. Phys. **A444**, 154 (1985).
10D. J. Hinde *et al*., Proceedings of the Tours Symposium on Nuclear Physics, Tours, France, 1997; D. J. Hinde *et al*., Phys. Rev. C **60**, 054602 (1999).
11C. R. Morten *et al*., Phys. Rev. C **52**, 243 (1995); C. R. Morten *et al*., Phys. Rev. C **60**, 044608 (1999).
12W. Reisdorf *et al*., Nucl. Phys. **A438**, 212 (1985).
13H. Timmer *et al*., Nucl. Phys. **A633**, 421 (1998).
14L. C. Vaz and J. M. Alexander, Phy. Rep. **69**, 373 (1981).
15C. L. Jiang *et al*., Bull. Am. Phys. Soc. **42**, 1043 (1997).

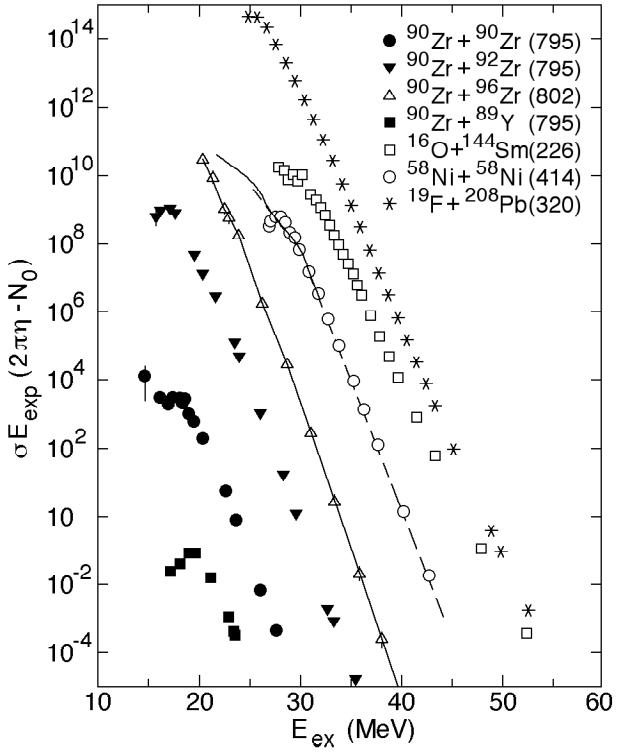

Fig. I-55. S(E) · exp(-N_0) plots as functions of the excitation energy E_{ex} of the compound nucleus for the systems $^{90}Zr + ^{90}Zr$, ^{92}Zr, ^{96}Zr, ^{89}Y, $^{16}O + ^{144}Sm$, $^{58}Ni + ^{58}Ni$, and $^{19}F + ^{208}Pb$. The measured cross sections are from Refs. 6,7,8,11. The parameter N_0 is an arbitrary normalization constant, which is given in the parenthesis.

Table 1: Energies E_0 and cross section sigma(E_0) determined from the bend-over in the S-factor. The excitation energy of the compound nucleus at E_0 and the predicted barrier height B_{Vaz} (Ref. 14) are also shown.

System	E_0	E^*_{CN}	B_{Vaz}	σ(E_0)	Ref.
MeV	MeV	MeV	mb		
^{90}Zr + ^{90}Zr	176.0	18.7	191.1	0.13	[6]
^{90}Zr + ^{92}Zr	171.5	17.6	190.4	0.014	[6]
^{90}Zr + ^{89}Y	171.1	19.6	186.2	0.29	[6]
^{16}O + ^{144}Sm	58.84	30.2	61.50	10.2	[7]
^{58}Ni + ^{58}Ni	93.88	27.7	101.5	0.35	[8]
^{16}O + ^{154}Sm	52.41	36.0	60.60	0.18	[7]
^{86}Kr + ^{92}Mo	158.6	20.5	180.3	0.007	[9]
^{86}Kr + ^{104}Ru	162.5	22.4	185.8	0.0049	[9]
^{19}F + ^{208}Pb	75.11	25.0	85.60	0.023	[11]
^{16}O + ^{208}Pb	70.13	23.6	76.62	0.39	[10]
^{40}Ar + ^{144}Sm	116.6	25.8	145.2	0.0016	[12]
^{40}Ar + ^{112}Sn	96.60	33.5	121.2	0.0084	[12]
^{40}Ca + ^{90}Zr	94.05	36.7	101.7	0.84	[13]

d.27. Yield Calculations for an Advanced Rare Isotope Accelerator Facility (C. L. Jiang, B. Back, I. Gomes, A. M. Heinz, J. Nolen, K. E. Rehm, G. Savard, and J.P. Schiffer)

The design of the Rare Isotope Accelerator (RIA) facility, requires the calculation of estimates of optimal yields for a variety of reaction mechanisms over a range of energies and beam-target combinations.

The yield calculations were refined over the past year and extended to the level of 10^{-4} particles/sec, that might be adequate for some experiments. These calculations were carried out in the perspective of the Recommendations of the ISOL Task Force Report to NSAC[1] for a 100 kW, 400 MeV/u accelerator, both for beams reaccelerated to precise low energies, and for prompt, fast fragmentation beams. During the past year many improvements were implemented in the computer codes that were developed previously.[2,3]

1. In-Flight Projectile Fragmentation

- A database for the cross sections calculations for projectile fragmentation was created using the Code EPAX[4]. Recently a new version of EPAX was published.[5] This new version, however, overpredicts the cross sections for projectile fragmentation of uranium beams which were measured in Refs. 6 and 7. By modifying the phenomenological parameters used in EPAX for beams of ^{238}U and ^{232}Th, good agreement with the experimental data was achieved. These modified parameters were then used in the calculations.

- The momentum acceptance of the recoil separator for fragmentation products is assumed to be ±9% and ±3% for the re-accelerated beams and the fast beams respectively. The extraction efficiency of the gas cell (stopper) was taken as 20% and an upper limit of 10^9 particles/sec was assumed, since it is not known whether higher intensity 1^+ beams can be extracted from the gas stopper. No such upper limit was assumed for fast projectile fragments.

- The influence from secondary reactions was previously included. Contributions from higher order reactions were considered for higher beam energies. A calculation for the $^{40}\text{Ar} + {}^{9}\text{Be} \rightarrow {}^{19}\text{C}$ reaction is shown in Fig. 1-56. These contributions are plotted as functions of the target thickness (dash lines). The ten thin vertical lines indicate the target thicknesses that can be used for beam energies of 100 - 1000 MeV/nucleon respectively, which are restricted by the momentum acceptance of the recoil separator (±9%) mentioned above. The solid curves represent the predicted yields including primary, primary + secondary processes etc., here attenuation effects are also included. As can be seen from Fig. I-56, at 1000 MeV/nucleon incident energy even third order effects have to be included. The higher order contributions have their biggest influence for the most neutron-rich isotopes. These higher order effects will be studied experimentally in an upcoming experiment at GSI.[8]

2. Spallation (Standard ISOL)

- The data base for proton induced spallation reactions was created using the CERN data base for E_{proton} = 600 and 1000 MeV measurements.[9] In some cases the database was extended towards the dripline by extrapolations. The extraction efficiency for the reaction products in the standard ISOL method depends very strongly on the chemical properties and on the lifetime of the isotopes. We used the parameters of Rudstam et al.[10] for the calculations of the extracted yields. For cases where no data for lifetimes were available, the estimates from Ref. 11 were used.

- In some cases spallation by heavier nuclei produces higher yields, e.g. for the case of Fr isotopes, that are best produced by spallation of ^{232}Th with ^{3}He beam. These are included in the calculations. Such spallation calculations have not yet been done systematically for all isotopes. Compound nuclear reactions might also be important in some cases,[12] but have so far not been included in the compilation and calculations.

3. Fast Neutron Induced Fission

The database for fast neutron induced fission mechanism was calculated from the Monte Carlo code LAHET.[13,2] Since calculations of processes with very small cross sections with this code are quite time consuming, the data base was extended by extrapolations. The extraction efficiency for the reaction products here is similar to the standard ISOL method. The corrections for the appropriate extraction efficiency due to the lifetime of the isotopes were also applied.

4. In-Flight Fission

For in-flight fission reactions, the database comes from experiments induced by a 750 MeV/nucleon ^{238}U beam at GSI,[14] and from calculations with the Abrasion-Ablation Model[15] on the proton rich side of the mass valley. The cross sections were assumed not to change appreciably within this energy range. Yields for nuclei close to the drip lines were obtained by extrapolations. The acceptance of the recoil separator and the extraction efficiency were given above.

Results

Fig. I-57a-c shows the yields for various Kr isotopes produced at a 100 kW, 400 MeV/nucleon machine. Intensities for re-accelerated beams produced by different methods are shown by different colors and symbols in Fig. I-57a. Yields obtained by extrapolating experimental data are indicated by open symbols. The optimal yields obtained for re-accelerated beams by any one of the different methods is shown in Fig. I-57b. Fig. I-57c presents the optimal yields that are available for fast beams (200 - 300 MeV/nucleon). On the neutron rich side the yield at first decreases exponentially as the neutron number increase, then it decrease more slowly. This is due to the secondary reaction contributions but remains to be confirmed. Similar plots are available for all elements, from helium to uranium.

Two dimensional contour plots of the yields in the N-Z plane calculated for RIA (100 kW, 400 MeV/nucleon), for 1^+ ions extracted from the ion source or the gas stopper cell are shown in Fig. I-58a-b. Fig. I-58a shows which of the four production mechanisms gives the optimal yield. It is clear that the in-flight fission and two-step fission mechanisms are very important for the production of neutron rich nuclides. The spallation mechanism provides the strongest beams (up to 10^{12}/sec) especially in the vicinity of the stable isotopes, while fragmentation can produce any nuclide independent of its chemistry. Fig. I-58b shows the yields in the N-Z plane available for re-accelerated beams, while Fig. I-58c is the result for high energy (~150 - 350 MeV/nucleon) beams. These plots extend to isotopes for which the yield would be on the order of a few counts per day (10^{-4} particles/sec). These yield-calculations are also available on the web.[16]

---

1 ISOL Task Force Report to NSAC, November 22, 1999. See http://srfsrv.jlab.org/isol/.
2 C. L. Jiang, B. Back, I. Gomes, A. M. Heinz, J. Nolen, K. E. Rehm, G. Savard, and J. P. Schiffer, Physics Division Annual Report 1999, Argonne National Laboratory, page 11; Physics Division Annual Report 1998, Argonne National Laboratory, page 13.
3 Concept for an Advanced Exotic Beam Facility Based on ATLAS (1995); Report to Users, ATLAS Facilities, March, 1999, ANL-ATLAS-99-1.
4 K. Sümmerer, W. Brüchle, D. J. Morrissey, M. Schädel, B. Szweryn, and Y. Weifan, Phys. Rev. C **42**, 2545 (1990).
5 K. Sümmerer and B. Blank, Phys. Rev. C **61**, 034607 (2000).
6 M. Pfutzner, Phys. Lett. **B444**, 32-37 (1998).
7 A. R. Junghans, DISS. **98-07**, March 1998, GSI; A. R. Junghans *et al*., Nucl. Phys. **A629**, 635 (1998).
8 G. Savard *et al*., Proposal **S258**, GSI PAC, December 2000.
9 Netscape, ISOL Task Force Information, CERN-ISOLDE part; J. Lettry, *et al*., Nucl. Instrum. Methods **B126**, 138 (1997).
10 G. Rudstam *et al*., Radio Chimica Acta **49**, 155 (1990).
11 P. Möller *et al*., At. Data Nucl. Data Tables **66**, 131 (1997).
12 W. Mitag *et al*., Nucl. Phys. **A616**, 329 (1997); M. Lewitowicz *et al*., Phys. Lett. **B332**, 20 (1994).
13 R. Alsmiller *et al*., Nucl. Instrum. Methods **A278**, 713 (1989).
14 C. O. Engelmann, Kernspaltung Relativistischer Uranprojectile und Erzeugung Extrem Neutronenreicher Isotope, Diss. **98-015**, 1998, GSI.
15 J. J. Gaimard, K. H. Schmidt, Nucl. Phys. **A531**, 709 (1991); J. Benlliure *et al*., Nucl. Phys. **A660**, 87 (1999); T. Enqvist *et al*., Nucl. Phys. **A658**, 47 (1999).
16 See http://www.phy.anl.gov/ria/index.html.

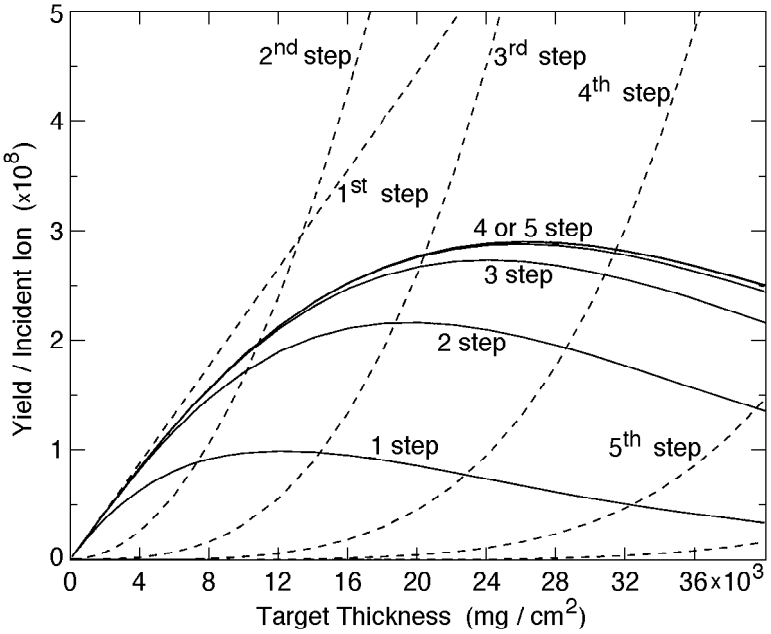

Fig. I-56. Contributions from higher order processes to projectile fragmentation in the system $^{40}Ar + {}^{9}Be \rightarrow {}^{19}C$. The solid lines give contributions including primary, primary + secondary effects, etc. Attenuation effects in the thick targets are also included.

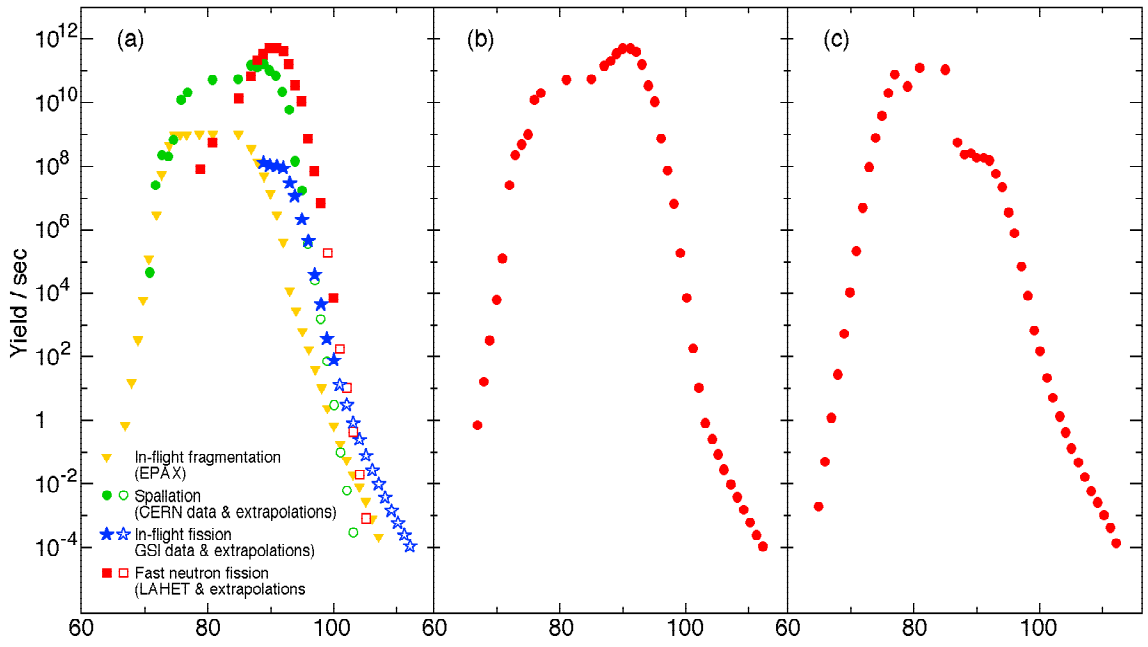

Fig. I-57. Production yields as function of the mass number for Kr isotopes produced at a 100 kW, 400 MeV/nucleon facility. a: Yields for re-accelerated beams obtained from different production methods are indicated by different colors and symbols. The open symbols were obtained from extrapolations of experimental data. b: Optimal yields that are available for re-accelerated beams. c: Optimal yields that are available at high energy (200 - 300 MeV/nucleon) beams.

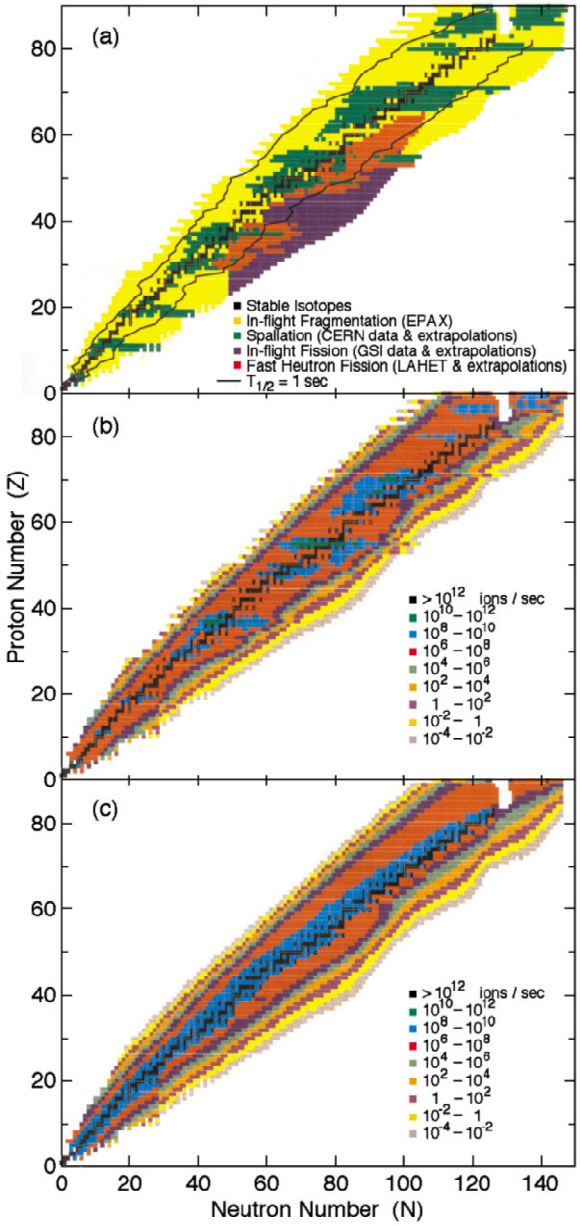

Fig. I-58. Contour plots for optimal yields as a function of N and Z produced at a 100 kW, 400 MeV/nucleon facility. a: Yields for re-accelerated beams obtained by different production methods are indicated by different colors. b: Yields for isotopes available for re-accelerated beams. c: Yields for isotopes available at high energy (150-350 MeV/nucleon) beams. These plots extend to isotopes for which the yield would be on the order of a few counts per day (10^{-4} particles/sec).